CAPITAL UNIVERSITY OF SCIENCE AND TECHNOLOGY, ISLAMABAD

Graphene Based Material for Supercapacitance Application

by

Arsalan Haider Noor

A thesis submitted in partial fulfillment for the degree of Master of Science

in the

Faculty of Engineering
Department of Electrical Engineering

2021

This thesis is dedicated to my Teachers, Parents and Family for their never-ending love, support, care and encouragement

CERTIFICATE OF APPROVAL

Graphene Based Material for Supercapacitance Application

by

Arsalan Haider Noor

Registration No: (MEE-181005)

THESIS EXAMINING COMMITTEE

S. No.	Examiner	Name	Organization
(a)	External Examiner	Dr. Shabbir Majeed Chaudhry	UET, Taxila
(b)	Internal Examiner	Dr. Muhammad Ashraf	CUST, Islamabad
(c)	Supervisor	Dr. Noor Muhammad Khan	CUST, Islamabad

Dr. Noor Muhammad Khan
Thesis Supervisor
April, 2021

Dr. Noor Muhammad Khan
Head
Dept. of Electrical Engineering
April, 2021

Dr. Imtiaz Ahmed Taj
Dean
Faculty of Engineering
April, 2021

Author's Declaration

I, **Arsalan Haider Noor,** hereby state that my MS thesis titled "**Graphene Based Material for Supercapacitance Application**" is my own work and has not been previously submitted by me anywhere else for taking any degree. At any time if my statement is found to be incorrect even after my graduation, the University has the right to withdraw my MS Degree.

(Arsalan Haider Noor)

Registration No: (MEE-181005)

Plagiarism Undertaking

I solemnly declare that research work presented in this thesis titled "**Graphene Based Material for Supercapacitance Application**" is exclusively my research work with no remarkable contribution from any other individual. Small contribution/help wherever taken has been dully acknowledged and that complete thesis has been written by me.

I understand the zero tolerance policy of the Higher Education Commission and CUST towards plagiarism. Therefore, I as an author of the above titled thesis declare that no part of my thesis has been plagiarized and any material used as reference is properly cited.

I undertake that if I am found guilty of any formal plagiarism in the above titled thesis even after award of MS Degree, the University reserves the right to withdraw/revoke my MS degree and that HEC and the University have the right to publish my name on the HEC/University website on which names of students are placed who submitted plagiarized work.

(Arsalan Haider Noor)
Registration No: (MEE-181005)

Acknowledgement

All praises be to Allah Almighty for blessing me with intellect, stamina, and courage to complete my work in time. Nothing would have been possible without His grace.

I wish to express my sincere gratitude to **Dr. Noor Muhammad Khan**, my supervisor for guidance, support, and valuable cooperation throughout the course. He has played a pivotal role in accomplishment of this project. I am also thankful to **Dr. Naseem Iqbal** for guidance, support and help especially with the material, analysis and characterization.

I am thankful to my thesis examination committee members for their assistance, kindness and guidance. I am thankful to Department of Electrical Engineering, Capital University of Sciences and Technology (CUST) and USPCAS-E, NUST for facilitating me with the lab facilities.

I am grateful to Allah for blessing me with the family who has always backed me and has given me the courage, love and support that I needed. I am thankful to my parents and siblings for always pushing me ahead.

Arsalan Haider Noor

Abstract

Supercapacitors are gaining attention day by day due to their intrinsic characteristics such as high power density and superior cyclability in contrast to batteries. Electrochemical double layer capacitors (EDLCs) are utilized as significant storage technology for electrical energy which will play vital role in development on large scale non-steady renewable energy sources, electrical vehicles, and smart power stations. It was observed that increased surface area, high porosity and activated carbon enhance the capacitance and charge-discharge rates of EDLCs along with electrical conductivity. Metal-organic frameworks (MOFs) in this regard, serve as a material having far more surface area than that of activated carbon. In this research work, three composite materials of reduced graphene oxide(rGO) with metal organic frameworks (MOFs) of cobalt, nickel and copper have been synthesized by using solvothermal process. The composites of rGO with metal organic frameworks were prepared by using metal precursors and benzene tricarboxylic acid (BTC) as a linker and 5wt% of reduced graphene oxide (rGO). The prepared materials were characterized by XRD, FTIR, SEM and EDX techniques to investigate the successful synthesis of rGO/MOF composites and to determine their structural and morphological properties. The electrochemical analysis for supercapacitor application was performed via cyclic voltammetry, electrochemical impedance spectroscopy and chronopotentiometry. Among the three synthesized reduced graphene oxide/MOF based composites as electrode materials, the reduced graphene oxide/copper composite shows the specific capacitance of 60.92 F/g in 2M KOH electrolyte solution and the energy density of 4.87 Wh/Kg. The second composite electrode material namely reduced graphene oxide/nickel composite demonstrate specific capacitance of 542.34 F/g in 2M KOH electrolyte solution and the energy density value of 43.38 Wh/Kg. The third sample viz. reduced graphene oxide/cobalt composite exhibits highest specific capacitance up to 562.12 F/g in 2M KOH electrolyte solution and the energy density value of 44.96 Wh/Kg.

Contents

List of Figures

List of Tables

Abbreviations

AC	Alternating Current
BDC	Benzene Dicarboxylate
CV	Cyclic Voltammetry
CA	Chronoamperometry
CE	Counter Electrode
CNTs	Carbon Nanotubes
CD	Current Density
EIS	Electrochemical Impedance Spectroscopy
FTIR	Fourier Transform Infrared Spectroscopy
GO	Graphene Oxide
GDP	Gross Domestic Productivity
MOF	Metal Organic Framework
MOR	Methanol Oxidation Reaction
MFC	Microbial Fuel Cell
MCFC	Molten Carbonate Fuel Cell
OER	Oxygen Evolution Reaction
ORR	Oxygen Reduction Reaction
PAFC	Phosphoric Acid Fuel Cell
PEMFC	Polymer Electrolyte Membrane Fuel Cell
RE	Reference Electrode
rGO	reduced Graphene Oxide
SOFC	Solid Oxide Fuel Cell
SEM	Scanning Electron Microscopy
XRD	X-ray Diffraction

Chapter 1

Introduction

In the introduction chapter, the first section 1.1 gives an insight into various energy storage and conversion devices such as fuel cells, batteries, solar cells and capacitors. The second section 1.2 gives a brief overview of capacitors, supercapacitors, their types and components along with supercapacitor applications in various fields. The third section 1.3, provides a preface of materials used in this research work, such as Metal Organic Frameworks (MOFs) as well as its composites which are employed as electrode materials in supercapacitor application. In the fourth section 1.4, the details regarding the background of various characterization techniques are briefly presented and in the last section.

1.1 Energy Storage Devices

In the modern era life, electrical energy plays a very vital role to meet the present living standards. With each passing decade, natural fossil fuel resources are being depleted, so there is a high need for a transition towards electric power based vehicles and domestic consumption to meet the future challenges of everyday life.

Moreover, very high consumptions of fossil fuels over the past few decades lead to catastrophic climate changes due to the evolution of greenhouse gases, which can be averted by moving toward clean energy generation, storage and utilization.

Electrical energy is an incredibly versatile form of energy that can be used for transportation as well as to power homes and industry, but it suffers a major drawback in terms of its storage i.e. it's relatively challenging to store electric energy in a short span of time.

Among various known electrochemical energy storage devices are fuel cells, batteries, solar cells and supercapacitors. Fuel cells operate with hydrogen mainly as a fuel but hydrogen is the secondary source of energy itself and it is not available in nature. Apart from hydrogen generation from natural resources, storage of hydrogen also poses a big challenge, which leads to the high cost of this energy technology.

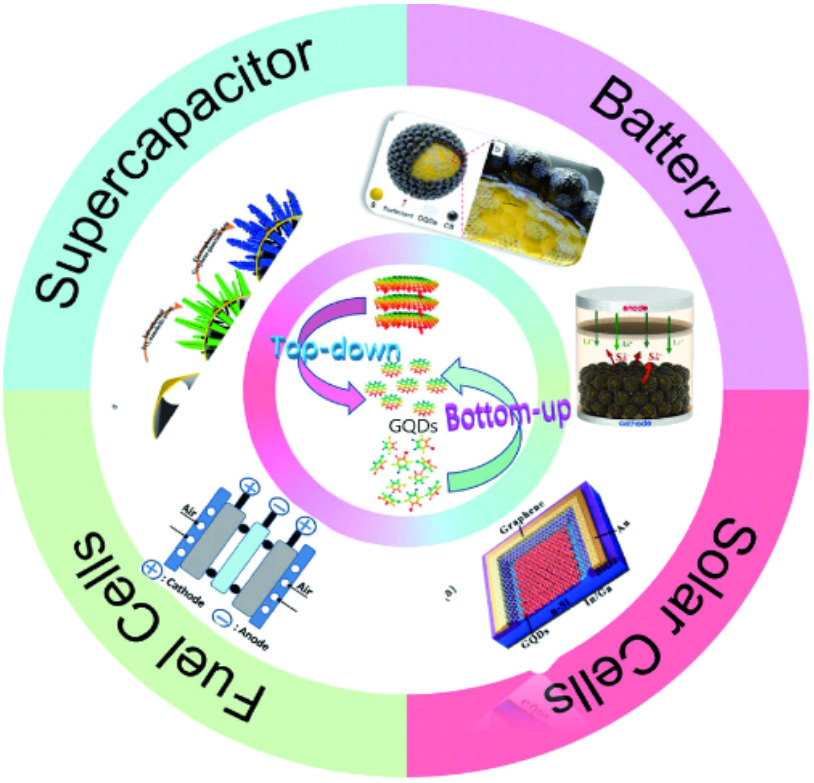

FIGURE 1.1: Electrochemical Energy Storage Devices

Solar cells, also known as photovoltaic cells are electric devices that work on the principle of converting light energy directly into electrical energy by making use of the photovoltaic effect. In this technology, the bottle neck is quantum efficiency as well as durability of the solar cells devices due to prolonged exposure to harsh ultraviolet light. These photovoltaic cells can degrade over a period of time

and therefore lose their quantum efficiency, particularly on exposure to extreme climates such as high temperatures in deserts and low temperatures close to poles.

The battery is an electrochemical device that comprises of single or combination of multiple electrochemical cells along with external connectors. They are used to power various electrical devices such as laptops, electric vehicles, cell phones etc. Batteries can store a significant amount of electric energy, but these devices can take up to hours for their charge up. There is also various hazard associated to their use such as leakage of corrosive chemicals, ingestion of battery and use of toxic material as their electrode or electrolyte like mercury, lead and cadmium metals. Capacitor are an electrochemical storage device that can get charge practically instantaneously, and can store a significant amount of energy.

1.2 Capacitors

At the beginning of electro technology, technologies used for storage of energy could be classified as (1) Inductors: which used magneto static field for energy storage, (2) Batteries: which undergo chemical reactions for energy storage, and (3) Capacitors: which used the electrostatic field for energy storage. Capacitors are one of the basic building units of electronic circuits. A capacitor is a passive device which contains two electric terminals and used for electrostatic energy storage. There are many different types of capacitors, but all of them comprise two electric conductor plates which are separated by a dielectric material. A variety of materials can be used as capacitors, for instance, metals thin films or foil of aluminum or disks. A dielectric having non-conducting nature acts to increase the charge capacity of capacitors. Although capacitors have existed for 2 centuries, advanced capacitor technology has only been known for 50 years. Many technologies are established for the development of advanced capacitors over half a century. Utility, industry, and transportation areas use polymer film capacitors which play a vital role in these areas. There is an increase in demand for lighter and smaller capacitors having high temperature capability in the power electronics industry, exploration

of gas and deep oil, military arena and hybrid vehicles. Using polypropylene and polyvinylidene fluoride as dielectrics, the metalizes film capacitors can offer an amount of 1–2 J/cm^3 energy density. A little improvement had been made until then in regard to high temperature capacitors with upto 200°C. There is a need to handle different operations at high temperatures for high temperature rating capacitors in pulse power system, gas and deep oil exploration, electric ships and military vehicles. One of the most complicated technological barriers in energy density has been identified is increasing temperature rating. For the development of better capacitors and related insulation would enable the operating system to work at temperatures ranges from 150–300°C that would be capable to achieve the light weight and miniature systems which will be the need of future.

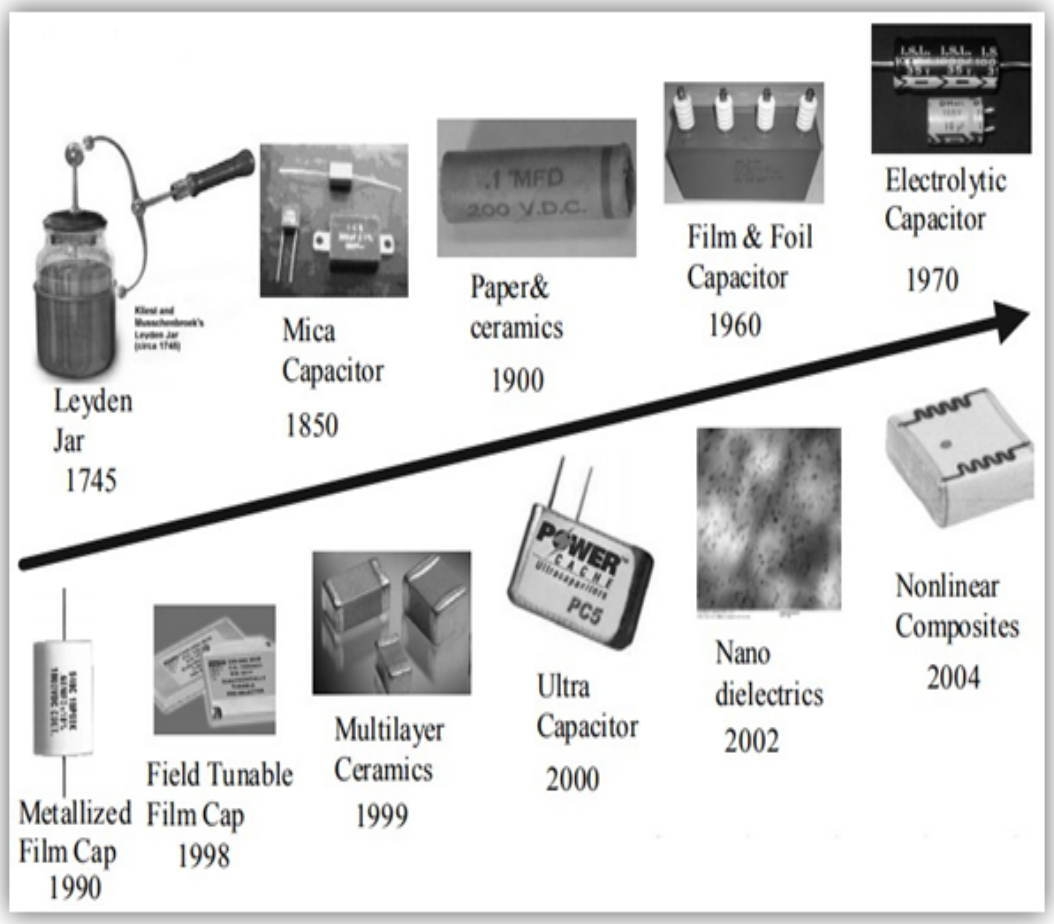

FIGURE 1.2: Development History of Advanced Capacitors

Traditional capacitors also called electrostatic capacitors, contain two conducting

electrodes divided by a dielectric. By applying an external voltage, charges try to assemble on two electrodes generating an electric field. The electric field allows the device to store electrical energy.

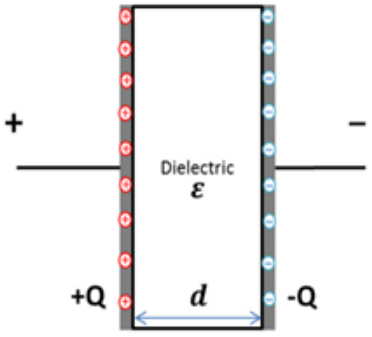

FIGURE 1.3: Illustration of an electrostatic capacitor

Capacitance is one of the significant characteristics of a the capacitor, which is the relation of the charge to the voltage:

$$C = \frac{Q}{V} \tag{1.1}$$

The capacitance will change by changing the voltage Under this condition, the capacitance can be presented as:

$$C = \frac{dQ}{dV} \tag{1.2}$$

For a capacitor comprising of two parallel plates with surface area, divided by a dielectric with permittivity, and a thickness, the voltage is described as the essential of the electric field with regards to the spacing:

$$V = -\int_0^d \xi dx = \int \int_0^d \frac{\rho}{\varepsilon} dx = \int_0^d \frac{Q}{\varepsilon A} dx = \frac{Qd}{\varepsilon A} \tag{1.3}$$

So, the capacitance can be represented as:

$$C = \frac{\varepsilon A}{d} \tag{1.4}$$

To attain high capacitance, the requirement is dielectric materials with better permittivity, reduce the spacing between two electrodes, and explore high surface area electrode materials. In literature [1-4], promising porous materials for electrodes are carbon with exceptional conductivity, like activated carbon, graphene, carbon aerogel and carbon nanotubes. The high surface area gives excellent charge storage ability in a small size packaged capacitor.

The primary features of an energy storage device are energy density and power density, with unit of energy or power per unit mass. The stored energy in a capacitor is represented as:

$$E = \frac{1}{2}CV^2 = \frac{Q^2}{2C} \tag{1.5}$$

To get the power density of a capacitor, the discharge time of the capacitor is desired.

$$P = \frac{E}{\Delta t} \tag{1.6}$$

Usually, power density values for capacitors are higher than 5000 W/kg, however value of energy density is low as between 0.01 and 0.05 Wh/kg. Capacitors are charged or discharged quickly as compared to batteries and fuel cells, however they cannot store a large quantity of energy.

Electrochemical supercapacitors are electrical energy storage devices both passively and statistically for those applications which require high power density for instance portable devices, hybrid automobiles and backup systems [5]. These electrochemical supercapacitors can store a significantly high amount of energy than regular conventional capacitors but lesser than batteries but their constructive framework is similar to the conventional capacitors with a difference in the material of metal electrodes which is placed by a highly porous electrode [6].

The capacitance values of a supercapacitor are high in electrochemical double layer capacitor devices [7]. The high capacitance of supercapacitors is because of the excellent electrochemically active surface area of electrode materials. Traditional supercapacitors are composed of highly active carbon material with a theoretical surface area of $\approx$ 1000–2000 m^2g^{-1} [8].

Electrochemical supercapacitors (ES) contain two electrodes, an electrolyte and a separator as shown in **Figure 1.4**. The most significant component of an electrochemical capacitor is the material of its electrode. Conventionally, the electrodes of supercapacitors are developed by nanomaterials which bear good surface area and porosity. It is clearly shown in **Figure 1.4**. that charges can be stored at the border between electrode material and electrolyte. This interface can be called a capacitor with EDLC and can be represented as follows:

$$C = \frac{A\varepsilon}{4\pi d} \tag{1.7}$$

Where, A = Surface area of the electrode (in case of supercapacitor it is an active surface of the electrode). ε = Dielectric constant of electrolyte. d = Thickness of the electrical double layer.

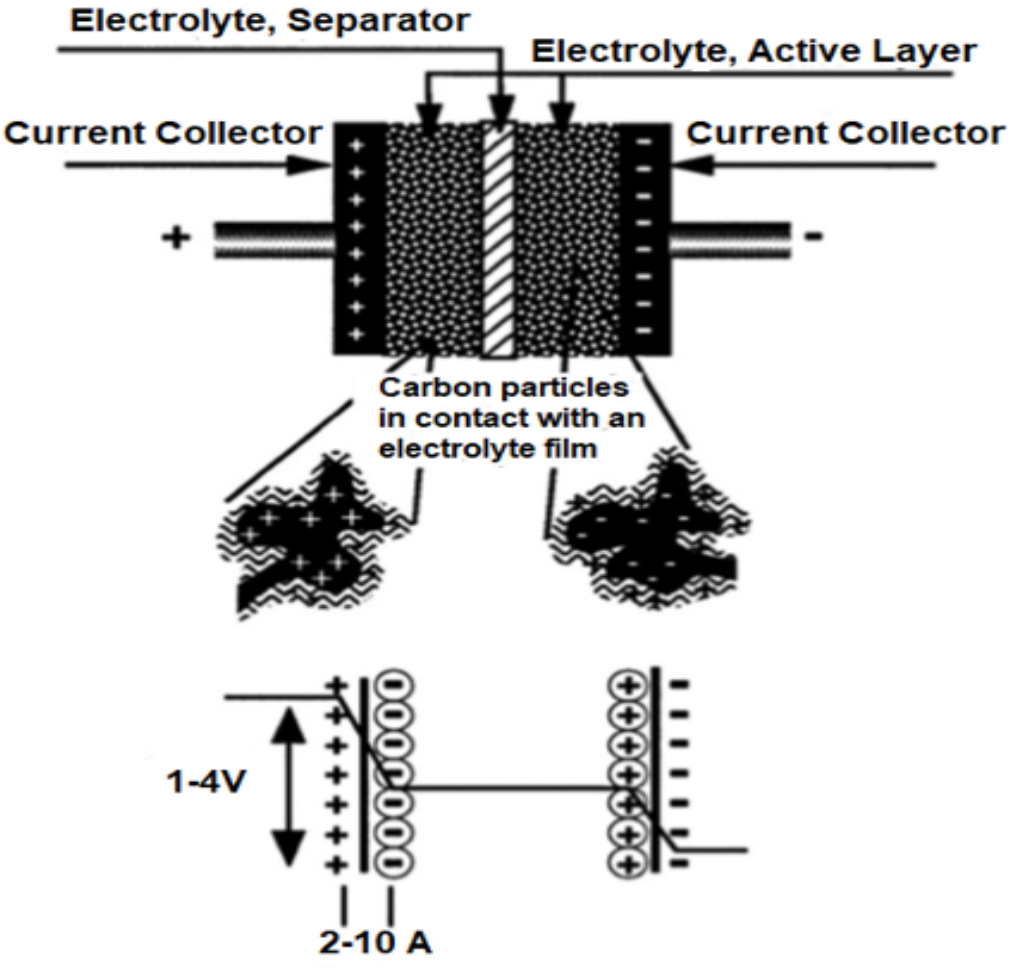

FIGURE 1.4: Electrical Double layer capacitor

1. **Electrical Double Layer Supercapacitor**

   In this type electrode material like carbon is not electrochemically active or there is no electrochemical reaction taking place on electrode material during the process of electrostatic charging or discharging and buildup of charges taking place pure physically at electrolyte interface.

2. **Pseudocapacitor**

   In this type electrode material is electrochemically active such as metal oxides that have the ability of charge storage during the process of charging and discharging [9, 10].

The electrolyte used in an electrochemical supercapacitor is categorized into three:

- Aqueous electrolyte
- Organic electrolyte
- Ionic liquids (ILs)

Often organic electrolytes are recommended because aqueous electrolytes have a larger limitation due to a small voltage window as low as 1.2 V which is very low as compared to organic electrolytes. While a number of electrodes and devices are also made by ionic liquids (ILs) electrolytes [11]. Electrochemical supercapacitors have various benefits like high power density, high efficiency, safer, long life, extend shelf life and wide temperature range. On the other hand, some challenges with ES like little energy density, cost, self-discharge and industrial standards for commercialization [12].

1.2.1 Principle of Conventional Capacitor

The traditional capacitor contains two electrodes and a separator which is insulating dielectric material is inserted. After applying voltage, positive and negative charges gather on electrodes. The dielectric separator is used to separate the charges [1].

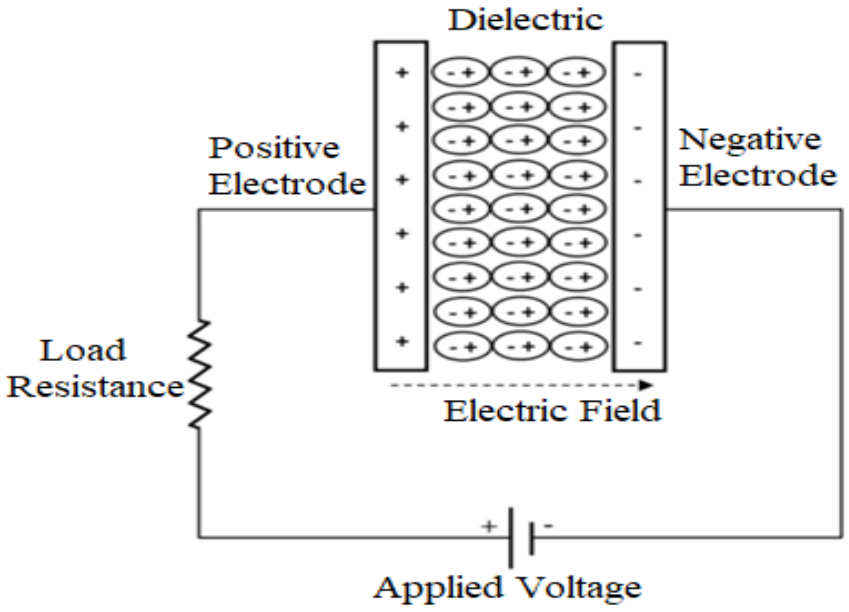

FIGURE 1.5: Schematic of a Conventional Capacitor

1.2.2 Supercapacitor

A new energy saving equipment that is conversion equipment such as supercapacitors is designed to partake the capability of high-power density, swift discharge-charge, excellent circulation facet, lacking self-discharging, safe in work, and low in cost. Various materials porous in nature are usually employed, such as metal organic frameworks, many carbon based composites of MOFs and many other composites i.e. (NiO and FeO based composites with carbon) are utilized for constructing supercapacitors due to their vast electrochemical features [13].

1.2.2.1 Principle of Supercapacitor

Mostly, the working principle of a supercapacitor is similar to conventional capacitors. Similar to the conventional capacitor, supercapacitors comprise two electrodes disconnected by an insulating dielectric separator. The main difference between the two types of devices is due to high surface areas of electrode material in supercapacitors as compare to conventional capacitors, and an electrolyte solution. The capacitance and energy increase intensely in supercapacitors due to greater surface area and lesser space between electrodes.

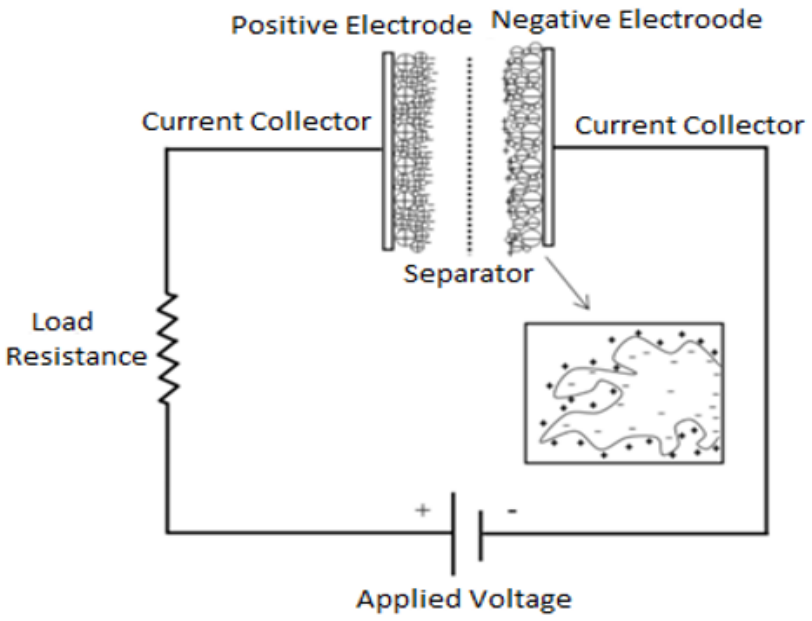

FIGURE 1.6: Schematic Diagram for a Double Layer Capacitor

1.2.2.2 Types of Supercapacitors

Supercapacitors are classified into two major types, namely electric double layer capacitors and pseudocapacitors. The major types as well as sub classes of supercapacitors are presented in Figure 1.7.

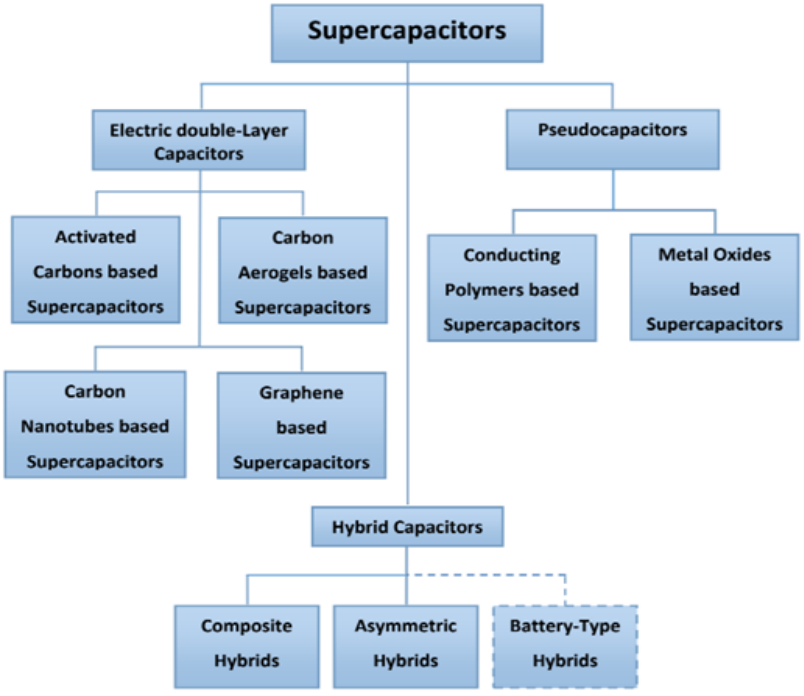

FIGURE 1.7: Types of Supercapacitors

1.2.2.3 Electrical Double-Layer Capacitors

Electrical double-layer capacitors (EDLC) consist of two electrodes system, an electrolyte for the conductance of ion, and a separator between two compartments. In electrical double-layer capacitors (EDLCs), charging and discharging are a greatly reversible phenomenon. This gives high cyclic stability for EDLCs. EDLC can store energy by means of an electrochemical double-layer of positive and negative charges when voltage is applied between electrodes. Voltage normally is lower than as compared to that required for a chemical reaction. Ions in electrolyte solution pass through the separator and arrive in voids of the electrode material. Due to applied voltages, charges start to gather at the electrode and electrolyte interface. However, ion recombination is avoided by the watchful design of the electrode material. From the initial development of EDLC, highly porous carbon electrode material with good surface area (SA), less costly and highly stable properties was used. Lately, many other kinds of carbon based materials were extensively used in EDLC, like activated carbons (AC), graphene, carbon aerogel and CNTs.

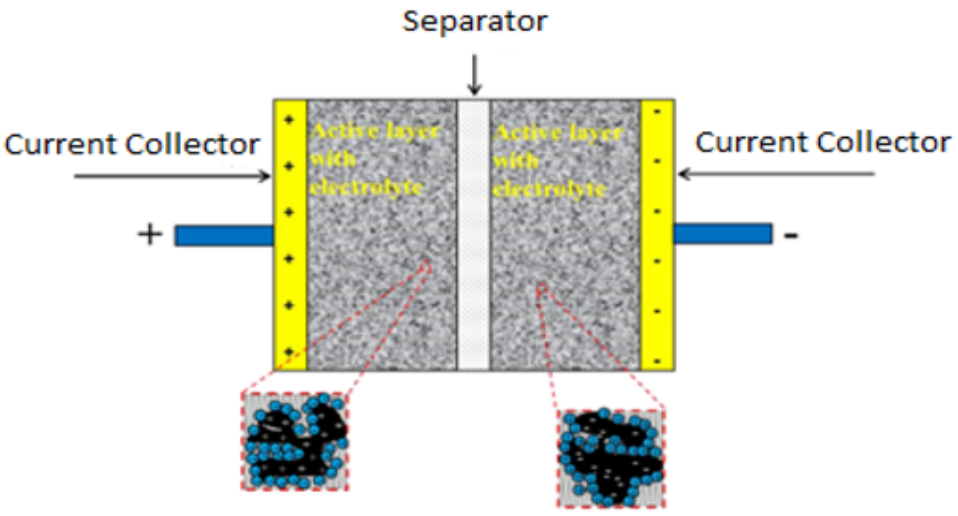

FIGURE 1.8: Diagram of a Charged EDLC

1.2.2.4 Pseudocapacitor

In pseudocapacitors, electric charge is stored due to redox reactions in electrode materials as compared to EDLCs where a charge is stored electrostatically. In

pseudocapacitors, to store charges different transition metal oxides and conducting polymers have been primarily employed [14, 15].

1.2.2.5 Hybrid Supercapacitors

Hybrid supercapacitors contain both double layer (carbon) and pseudocapacitance material (metal oxide) have appealed to substantial considerations [16]. The superior capacitance of hybrid supercapacitors is due to porous carbon materials and metal oxides [1]. Hybrid supercapacitors are of three types: 1) asymmetric, 2) composite, 3) battery-type.

Asymmetric have both EDLC and pseudocapacitor electrodes [17]. Asymmetric supercapacitors are better in cyclic stability as compare to pseudocapacitors. These types of supercapacitors can attain higher energy and power densities as compared to EDLCs. In composite supercapacitors, composite materials of carbon with metal oxides as electrode materials [18]. The carbon will provide a better surface area to increase the interaction of metal oxides with electrolytes [19-21].

1.2.2.6 Operational Voltages of Supercapacitors

Different supercapacitors have different voltage limits. The normal electrostatic capacitor can withstand high volts, while the supercapacitor can operate between 2.5–2.7 V. Higher than 2.7 V are possible but with reducing cycle life. To increase voltages, a series connection of supercapacitors is required. Internal resistance and capacitance are compromised in a series of connections of supercapacitors. A combination of more than three supercapacitors requires voltage balancing to avoid any cell from going into over-voltage.

1.2.3 Components of Supercapacitors

The design and components of the supercapacitors are like electrochemical batteries. The supercapacitors device parts comprise of:

i. Electrode

ii. Electrolyte

iii. Current collector

iv. Binder

v. Separators

The electrolyte and electrode are the active components of the supercapacitors. The current collector, binder and separator are considered inactive components of the supercapacitor. Generally, two current collectors are used with electrode materials [22].

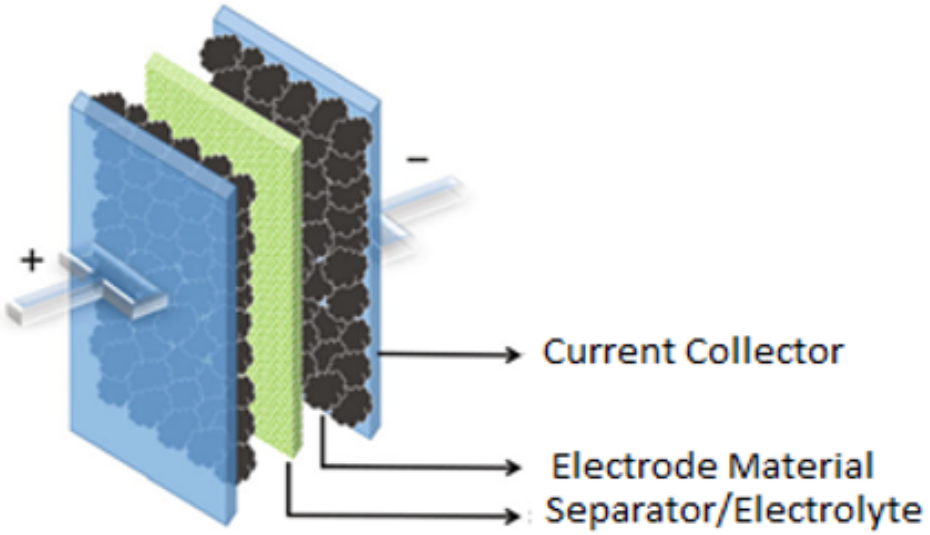

FIGURE 1.9: Components of Supercapacitors

1.2.3.1 Electrode Materials

In supercapacitors, electrode materials play a leading role in performance. Many electrode materials like carbon aerogels, activated carbon (AC), graphene and CNTs etc. illustrate the EDLC actions. Alternatively, the transition metal oxides are fall in the group of pseudocapacitive, in which storage of charges happens due to redox reaction (physio-chemical adsorption) on the surface of electrodes [23].

1.2.3.2 Electrolyte Materials

The prime challenge in supercapacitor development is to boost the values of energy density, which can be attained via enhancing the capacitance of electrode material or through broadening the device voltage window. Superlatively, expanding of voltage window can be beneficial for boosting the energy density of the device [13].

Moreover, cell potential sturdily leans on the electrolyte electrochemical stability used with the intention of evading parasitic and exhaustive reactions, therefore it is important to choose an appropriate electrolyte. Therefore, a range of different electrolytes in supercapacitors is available with adjustable voltage windows such as 1.0-1.3 V for aqueous electrolyte-based supercapacitors, 2.5-2.7 V for organic electrolytes-based supercapacitors and 3.5-4.0 V for ionic liquid supercapacitors. Furthermore, the electrolyte should have excellent activity, conductivity and resistance towards degradation [24]. Classification of electrolyte is shown in **Figure 1.10**.

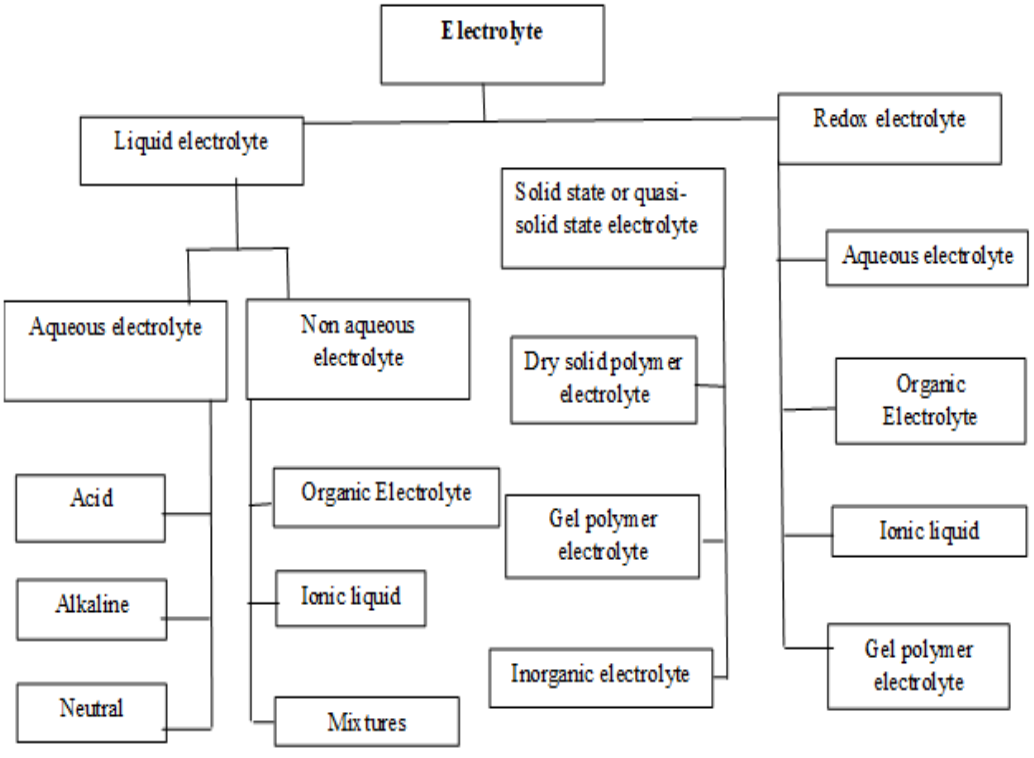

FIGURE 1.10: Types of Electrolytes for Supercapacitor

1.2.3.3 Current Collector

The active components of supercapacitors are electrolyte and electrode materials, while the passive component is the current collector. But, similar to the electrolyte and electrode materials, it performs an important role in the cell potential and durability improvement of a supercapacitor. The choice of a current collector exclusively is contingent on electrolyte and electrode such as metal foil (corrosion resistive) current collectors like gold have been utilized in strong acid-based electrolytes.

Additionally, to reduce the cost, indium tin oxide plates and carbon materials can be used. While supercapacitors are based on alkaline electrolytes, Ni materials are selected as an appropriate current collector due to low costs like Ni foam. Moreover, supercapacitors are based on non-aqueous electrolytes, the broadly used current collectors are aluminum [25].

1.2.3.4 Binder

Binders have been utilized with a milled electrode material that will not only help in the maintenance of structure but also assist in attaining an improved connection between the current collector and active material. Normally, polymeric materials like PVDF, PVP, PAA, PTFE, natural cellulose, Nafion, and polyaniline (conductive polymers) have been used as a binder.

Though, the presence of binders in surplus quantity could have a constraining effect on the performance of supercapacitor because of their aquaphobic property that obstructs the penetration of electrolyte may lead to reduce capacitance performance. In several cases, the binder's mixture in an optimized amount has been applied to obtain more electrolyte access and more wettability. Attributable to the adversative effects such as lessened active surface, lower conductivity and electrode materials wettability, utmost existing technologies of supercapacitor are targeting to prepare binder free electrodes, that bring about electrode material improved electrochemical activity [26].

1.2.3.5 Separators

Like binders and current collectors, the separator is an inactive part of supercapacitors. Though it has not any impact on the efficiency of the supercapacitor but does an essential part by stopping connection in between electrodes and assisting electron transferal.

i. electrical insulator

ii. elevated mechanical strength

iii. chemical/electrochemical inert

iv. ion transfer capability

v. porosity

vi. width

vii. Surface morphology.

A range of separators is fabricated by a broad range of materials such as PTFE, PP, PVDF, cellulose polymer membranes, glass fiber, films of graphene oxide and Nafion etc [27].

1.2.4 Applications of Supercapacitors

Supercapacitors have the capability to deliver more power as compare to electrochemical batteries and store a large amount of energy in contrast to traditional capacitors.

1.2.4.1 Consumer Electronic Products

1.1.4.1.1 Backup Power Sources Supercapacitors can be employed as backup power in microcomputers, memories, and electronic boards [28, 29].

In a backup power application, the main power source will be a typical load.

1.1.4.1.2 Main Power Sources

Supercapacitors supply one or numerous large current pulses of short duration (ms). These supercapacitors can be installed as the main power source for many applications. For example, in a toy car, the battery can charge these supercapacitors or chargers in the "rechargeable motors" [29]. These supercapacitors very fast in charging and provide power for acceleration. A low power rating can also be used for charging these supercapacitors.

1.1.4.1.3 Alternate Power Sources

Supercapacitors can be used in different alternate power source applications. In a solar PV system, during the daytime, in addition to supply electric load, these supercapacitors are charged by the solar system. Similarly, in the solar watch concept, the solar cell can charge a supercapacitor and can provide power to watch for a longer time [29]. This type of system is reliable and long life without maintenance.

1.2.4.2 Vehicles Applications

Supercapacitors are used in electric vehicles (EVs) and hybrid electric vehicles (HEVs), to provide high power for short time and to store regenerative braking energy. This type of application of supercapacitors can minimize the number of batteries or size of the internal combustion engine (ICE) [29]. The same type of combination can also be utilized in ships and aircraft.

1.2.4.3 Industrial Process

Few industrial processes are delicate to stoppages of the mains power, like chemical processes, textile industry and pharmaceutical industry processes. This interruption of the power supply is costly for the production industry. Supercapacitors can provide consistent energy to power these sensitive industrial processes.

1.3 Metal–Organic Frameworks (MOFs)

MOFs belong to highly porous with upto 90% free volume) class of materials that are incomparable not only in their physical and chemical characteristics but also in their diversity in structure and degree of versatility for both inorganic and organic components of their structure. MOFs also possess ultrahigh Brunauer-Emmett-Teller (BET) surface areas that are extending more than $\approx 7000\ m^2/g$. All these properties make MOFs utilized in their potential applications in energy cleaning, most vital role in storage media significantly for gases like methane and hydrogen gas and also as adsorbent with high capacity to fulfill various needs of separation. Some other fields gaining importance rapidly in the area of membranes which include catalysis, thin film devices and biomedical imaging. The contrast of two elements of metal organic framework, the metal ion cluster and the organic linker both provide an infinite number of possibilities. The possibly developed synergistic effect by the sum of physical properties of organic and inorganic components play a vital role in the characteristics of the whole MOF [30].

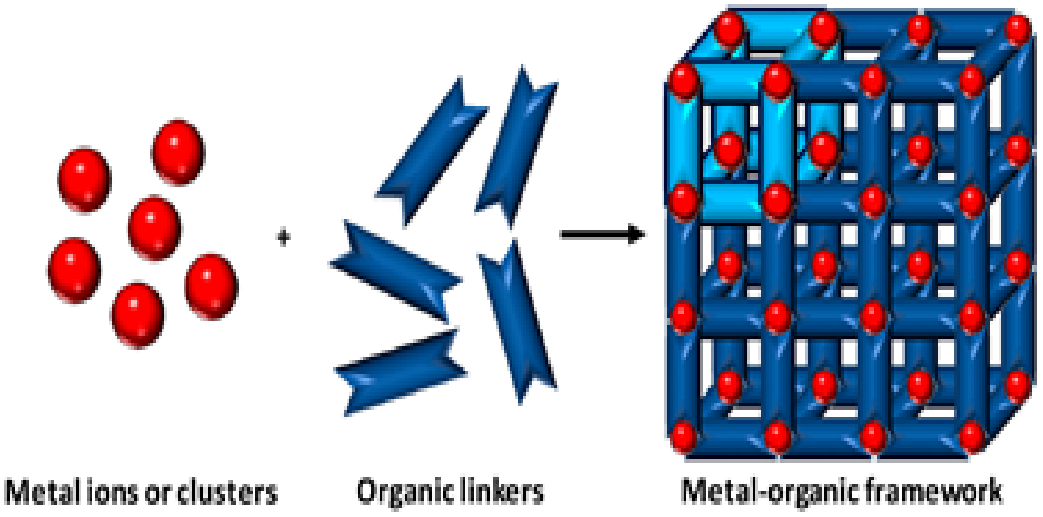

FIGURE 1.11: Metal-Organic Frameworks

Major characteristics of metal organic framework such as large surface area makes them promising candidate to use in catalytic applications for incorporation of active phases. In some cases, MOFs are additionally constructed by nodes of metal and aromatic linkers which can certainly develop charge transfer interactions by

coordination of $\pi - \pi$ forces which offer an additional advantage for improvement of activity of metal nanoparticles and its stabilization as compared to other supports such as mesoporous aluminosilicates and zeolites [31]. MOFs along with incorporated metal oxide nanoparticles can be assumed to construct the structure of metal organic framework around pre-formed nanoparticles [32]. The synthetic methods are usually composed of two steps. The first step includes a metal precursor which is introduced into the porous network for the first time and then this step is followed by the reduction process of the incorporated precursor and in the second step doe the generation of metal nanoparticles [33].

1.3.1 Ni-BTC Metal Organic Framework

Nickel based MOFs have got more interest due to their vast applications in the area of supercapacitors and also that these MOFs can be used as precursors for the formation of distinctive metal oxide and carbon materials with explicit structure [34] [35]. Ni-BTC MOF was at the beginning reported by Yaghi [36]. It is demonstrated that Ni-BTC MOF formed by the hydrothermal method has high specific capacitance with the value of 726 F/g [37].

The Synthesis process of Ni-MOFs normally needed plenty of solvents, high temperature and extended reaction time [38]. Effect of solvent on the formation of Ni-BTC was tested with different solvent mixtures such as water and dimethylformamide (DMF), water and ethanol, as well as a mixture of three solvents namely ethanol, water and DMF [39] [40].

1.3.2 Co-BTC Metal Organic Framework

As it was discussed that metal organic framework (MOF) being permanently porous materials possess immense current interest because of their low density and well-defined structures and their tremendous application potentials such as catalysis, gas storage and separation. Moreover, in this regard, polynuclear cobalt complexes have been the intensive subject of study due to owning their formation

of a variety of innovations in structural networks which include sheets, chains and matrices [41] [42].

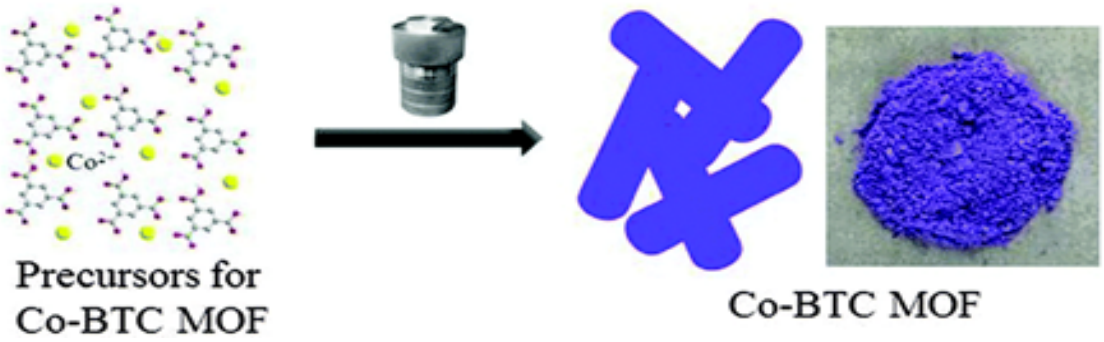

FIGURE 1.12: Synthesis of Co-BTC MOF

1.3.3 Cu-BTC Metal Organic Framework

$Cu_3(BTC)_2$ (BTC = 1,3,5-benzenetricarboxylate) which is also known as Cu-BTC and HKUST-1 or MOF-199 [43], is one of the well-known MOF which possess square shaped pores of size $9\mathring{A}$ by $9\mathring{A}$. This Cu-BTC MOF was reported by Williams and co-workers for the first time in 1999 [44]. The synthesis of pure phase Cu-BTC was quite difficult in the beginning due to the formation of side products such as metallic and oxidic copper species in the early solvothermal procedure [45]. Several optimized routes such as electrochemical methods, high-throughput screening [46], ultrasonic [47] and microwave assisted procedures [48] have opened various possibilities for large scale production of Cu-BTC which a significant need of the hour for catalytic applications.

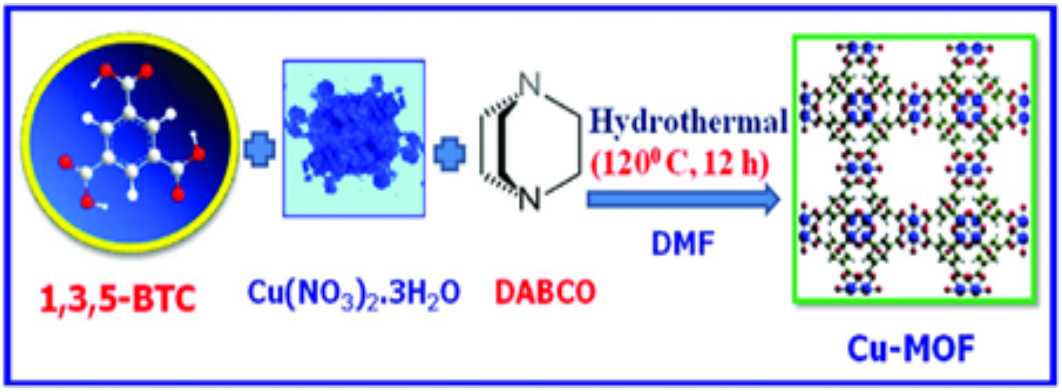

FIGURE 1.13: Synthesis of Cu-BTC MOF

1.4 Characterization Techniques

Samples characterization was carried out via FTIR, XRD and SEM techniques.

1.4.1 Fourier Transform Infrared Spectroscopy

FTIR is an efficient method to study compound composition and internal structure by recognizing functional groups present in the studied compound. IR spectroscopy equipped with Fourier transform technique is an easy approach for sample characterization. It is used for the analysis of organic as well as inorganic compounds.

The basic components of FTIR are IR source, sample, interferometer, laser, mirrors and detector. The basic principle of FTIR technique is the change in the dipole moment of the molecule as a result of molecular vibrations when infrared radiations strike the molecule. The working principle of the instrument is that IR radiations from source strike to beam splitter and splitter beam transfer to the fixed and movable mirror. The moveable mirror reflects the beam to beam splitter from where it is focused on the sample and then response reaches a detector and the resultant spectrum is displayed on the monitor [49].

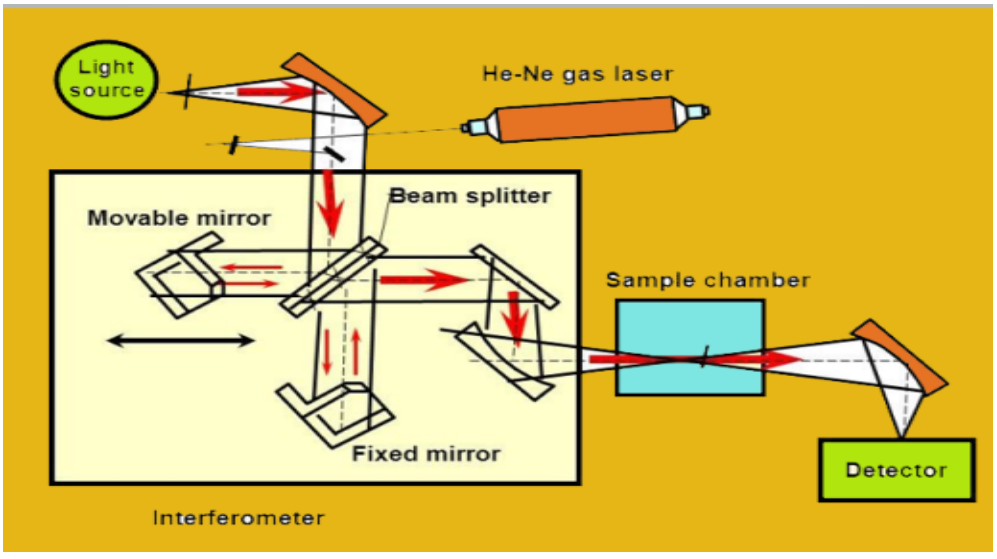

FIGURE 1.14: Construction and Working of Fourier Transform Infrared Spectroscopy

1.4.2 Scanning Electron Microscopy

SEM was developed first of all in mid of 19thcentuary by Max Knoll and a beam of an electron is utilized instead of the light source to develop an image of the material. SEM is easy to operate and information about topography, composition crystal structure and morphology are obtained within 5 minutes. Scanning Electron Microscope comprises of electron column equipped with an electron gun and electron lens, detectors, sample stage, vacuum and scanning system, electronic control and display system. The purpose of an electron gun is to instate and stimulate electrons to operate within 1-40 k eV range. Field emission and thermionic are two main types of an electron guns. Thermionic is mainly a material that is focused to an elevated temperature to eject an electron. In field emission, two electrodes are fixed and an electron is emitted from a metallic tip in the presence of magnetic field which is driven toward other electrode and then toward microscope in the presence of electric field by applying a voltage of 2 kV.

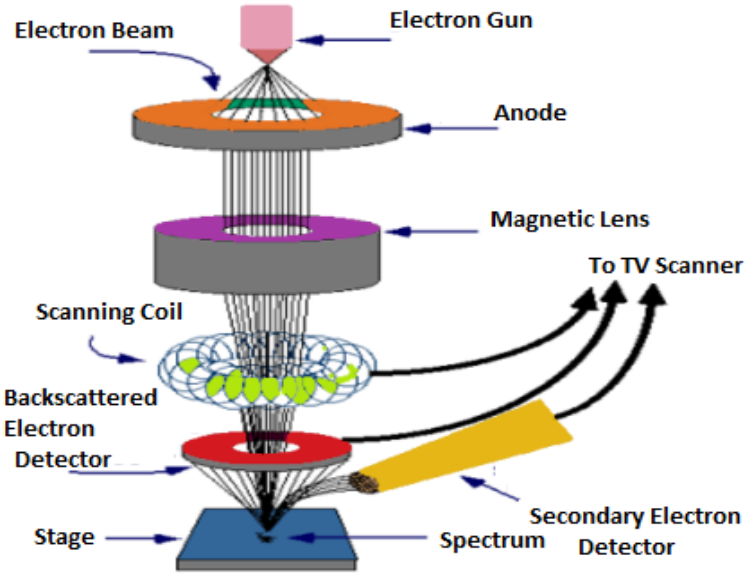

FIGURE 1.15: Instrumentation and Working of Scanning Electron Microscope

Electron beam focused by these anodes is further focused by a condenser lens and concentrated to form a probe. After concentration, an electron beam is passed through an aperture with electron exclusion. To avoid beam divergence stigmators are applied on the beam to fully focus on the sample. The beam received

by deflector coils is now thoroughly passed through the sample and information obtained from every part is transferred to monitor to get the final image [50].

1.4.3 X-Ray Diffraction

XRD is an excellent method for the study of the crystal lattice, crystal size, unit cell dimensions, atomic spacing and sample purity. X-Rays were discovered accidentally in by Roentgen in1895 while using a cathode ray tube. The main components of the XRD instrument are sample, x-ray tube, aperture, slits, goniometer, monochrometer, sample holder and detector. They are electromagnetic radiations that have the tendency of ionization and covered wavelength range is 0.01-10 nm [51].

$$n\lambda = 2dsin\theta \tag{1.8}$$

where, n= an integer showing the number of layers, λ= wavelength, D= interlayer spacing, θ = diffraction angle.

$$D = \frac{k\lambda}{\beta cos\theta} \tag{1.9}$$

Where, λ= wavelength, θ= diffraction angle, D= crystallite mean size (nm), β= Full width half maximum, k= Shape factor.

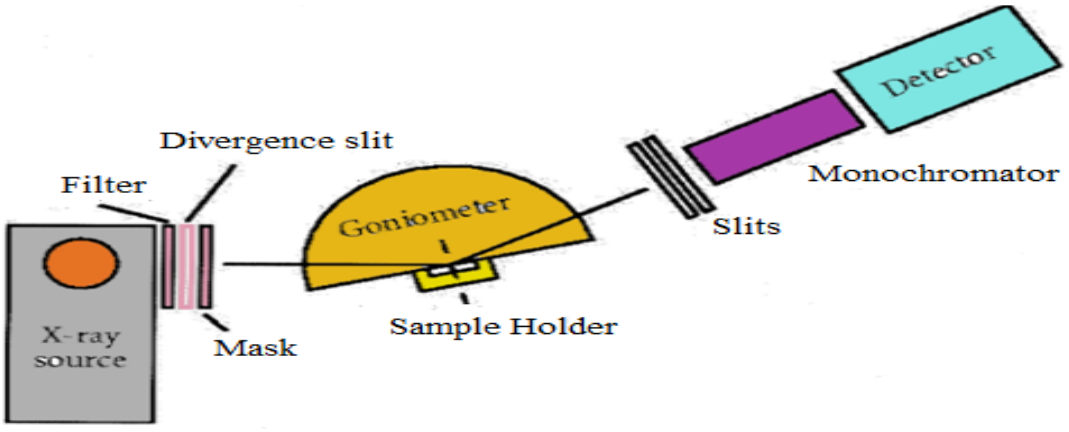

FIGURE 1.16: Basic Components and working principle of X-ray Diffractometer

1.5 Research Objectives

To overcome the supercapacitor research major obstacles that are elevated cost, as well as less density in terms of energy and improvements in existing technologies are required. Among synthesis of graphene, the methods that offer improved morphology and exfoliation which is also an economically viable process are desirable. Also, the fabrication technique that will be enabled to hold the highly porous electrode material and electrochemical properties of active supercapacitor electrode material for enhanced supercapacitance properties are required. The objectives of the present work are mentioned below:

- Synthesis of reduced graphene oxide composites with copper/nickel/cobalt
- Characterization of prepared samples by SEM, EDX, XRD and FTIR
- Electrochemical testing by Cyclic voltammetry, EIS and GCD for supercapacitor

Chapter 2

Literature Survey and Problem Statement

This chapter presents the literature review with a brief overview of the already reported electrode material used for supercapacitors. In the first part of this chapter section 2.1, an extensive study of previous approaches used for the development of electrode material in supercapacitors is discussed. The second part 2.2 presents the gap analysis in the area of supercapacitors research and also discusses the aim of this research. The third part 2.3 highlights the problem statement and the fourth part 2.4 presents propose research methodology and also about characterization technique used to investigate the physical and chemical properties of the electrode material. The last part also demonstrates the proposed plan to investigate the electrochemical performance of supercapacitor electrode materials.

2.1 Literature Review

In the recent decade, many researchers investigated many materials for supercapacitors. Yan et al. [2014] reported porous carbon that was synthesized from MOF-5. Being an electrode material, the MOF-5 derived porous carbons showed

potential capacitive behavior and demonstrated maximum specific capacitance of 232.8 F/g at 100 mA/g of current density in 30% KOH solution [54].

Hau et al. [2018] reported porous three NiO based material with a different surface area prepared from nickel-based MOF templates. Nickel oxides have an extraordinarily elevated theoretical specific capacitance and retain comparatively superior electrical conductivity in contrast to other metal based oxides. Though, the reported specific capacitance value for NiO-based electrodes is much lower than the theoretical value until now, because of the improved porosity, three NiO based electrode materials demonstrated an enhanced electrochemical activity and the discharge capacitances of 102, 105, and 116 Fg^{-1} at1 Ag^{-1} of current density. The specific capacitance of NiO is around 93.2% after 3000 cycles, which is better than earlier reported NiO electrode materials and recommended for their promising applications in supercapacitors[55].

Purkait et al. [2018] reported a network of rGO networks with copper wire that are used to assemble solid-state supercapacitor. An electrolyte such as polyvinyl alcohol/H_3PO_4 and exhibits specific capacitance of $81 \pm 3\ F/g$ energy density and power density respectively. The voltammogram showed cycling stability of 94.5% for 5000 cycles[56].

Shengtang Liu et al. [2018] reported nano films of TiO_2 coated with graphene-SnO_2 and graphene-Fe_2O_3 which depicts the exceptional electrochemical performance. Development of this facile and novel synthetic process offers the idea of graphene hybrids for batteries and supercapacitors [57].

Wenbo Yue et al. [2013] reported graphene-based metal oxides which possess a sandwich structure for Li-ion batteries. They used the stepwise heterocoagulation method for further protection of metal oxides by using nanosheets of graphene. These sandwiched materials of graphene-based metal oxides Co_3O_4 or possess higher reversible capacities in contrast to the conventional graphene-based material. For the alleviation of volume change of metal oxide during cycles it also acts as ideal strain buffers [58]. Wenyu Zhang et al. [2012] described one-step process for electrochemical production of graphene based nanostructure of metal oxides

for the storage of Li ions. Metal oxides were deposited, and sheets of graphene were separated in a single-step electrochemical process. High specific capacities showed by the hybrid electrodes with outstanding cycling stability. A discharge capacity of 894 $mAhg^{-1}$ was observed by Fe_2O_3/graphene anode. Co_3O_4/graphene showed discharge capacity of 880 $mAhg^{-1}$. The cathode of V_2O_5/graphene depicts 208 $mAhg^{-1}$ discharge capacity [59].

Hamid et al. [2016] reported nickel sulfide wrapped with graphene and utilized in Li-ion batteries and supercapacitors. Significant improvement of nickel sulfide was observed by graphene wrapping not only in the performance of Li-ion battery but also in the performance of supercapacitor electrode. The specific capacity of nickel sulfide wrapped with graphene as anode for Li-ion battery was observed above 1200 mAh/g cycles with improved rate capability. The specific capacity of nickel sulfide wrapped with graphene as supercapacitor electrode was observed around 1000 F/g and current density of 55A/g. It also improves the pseudocapacitive rate performance which enables nanocomposites to achieve high capacitance [60].

Xi'an Chen et al. [2014] reported the development of sulfur doped 3D porous hollow nanospheres framework of rGO and observed its performance both for supercapacitors and ORR. Moreover, this material depicts good rate capability, with excellent capacitance and better cycling stability. They believed that the reason for good performances is sulfur doping which enhances electrochemical performance which provides porous network structure. Furthermore, this type of material with its structural property may use as a conductive matrix in Li-ion, Li-S, supercapacitors, chemical sensors and catalysis [61].

Ke-Jing Huang et al. [2015] reported the successful fabrication of CuS-rGO composite. They used flexible rGO for wrapping of CuS hollow spheres. Furthermore, these composite bears the ability for the utilization of high conductivity, good mechanical property, large surface area and excellent electrochemical performance of rGO as well as extraordinary stability of hollow spheres of CuS. As the result shows, the composite of CuS-rGO depicts unusually high performance which further highlights the advantage of CuS possesses a special hollow structure and

combining rGO to reach the maximum performance for supercapacitors. They also propose to apply the same strategy to other hollow nanomaterials for the sake of enhancement of electrochemical performance for supercapacitors [62].

Wei Liu et al. [2018] reported metal sulfides with graphene composite for supercapacitors. The resultant composite also bears excellent mechanical integration and conductivity. It gives a high capacitance value of 310.2 C g^{-1} and shows an outstanding rate capability of 61.8% retention. The fabricated graphene composites depict high cycling stability over 10000 cycles [63].

Guangdi Nie et al. [2014] reported the successful synthesis of Bi2S3 with graphene oxide nanosheets composites (BGNS) which bear uniform morphology by using facile one-pot hydrothermal reaction using Sulphur compounds which serve as both sulfur source as well as reducing agent. The followed method could develop controlled fabrication of Bismuth graphene hybrids with adjustable size and composition can also be adjusted by the additive amount of graphene oxide. Adjustable composition and unique structure of nanohybrid also ensure effective electron transport and fast ion diffusion. Various advantages like an abundant resource, low cost and non-toxicity also prove Bismuth graphene hybrids as a promising material for practical application in supercapacitors [64].

Rajendran Ramachandran et al. [2015] reported the synthesis of ZnS with the decoration of graphene nanocomposites by using a facile solvothermal approach and confirm their successful synthesis by XRD, TEM, FTIR and UV spectroscopy. They use 6M KOH electrolyte for electrochemical measurements of different electrodes towards supercapacitor applications. A series of composites also prepared by adding different amounts of graphene and all the prepared composites were tested for electrochemical measurements. Cyclic voltammetry technique was used to evaluate specific capacitance with a value of 197.1 F/g using ZnS-graphene at a scan rate of 5mV/s. The capacitance retention is around 94.1% over 1000 cycles which suggest cyclic stability for a long time [65].

Weihua Cai et al. [2016] the synthesis of transition metal sulfides $NiCo_2S_4$ which were grown on fibers of graphene by using the solvothermal deposition method,

used for wearable asymmetric supercapacitors which bear high cell voltage with 1.5 V, high volumetric capacitance and high energy density in aqueous electrolyte. The selection of fiber is due to its light weight (0.24 gcm^3), flexibility, highly conductive and mechanically robust nature. The graphene based $NiCo_2S_4$ composite depicts high volumetric capacitance upto 388 Fcm^{-3} at 2 mVs^{-1} in a 3-electrode cell. The electrochemical measurements show higher capacitance of Graphene/$NiCo_2S_4$ in contrast to the pure fibers. The developed device obtains high energy density upto 12.3 $mWhcm^{-3}$ which also shows maximum power density with a value of 1600 $mWcm^{-3}$. So, the composites are promising candidates for wearable electronics and storage devices [66].

H. Tong et al. [2016] reported the fabrication of nanosheets of Zn Co sulfide on a film of graphene/carbon nanotubes (CNTs) material. Films of composite material serve as an electrodes and exhibit a high energy density of 50.2 $Whkg^{-1}$ at a power density of 387.5 Wkg^{-1} which shows 100% cycling stability over 2000 cycles [67].

Aming Wang et al. [2013] reported the controlled synthesis of novel nickel sulfide/-graphene oxide nanocomposites. The NiS gives a particle size of 50nm. Obtained results indicate an increase in conductivity by the addition of GO and also improve supercapacitance behavior of NiS/GO nanocomposites and the capacitance value of 800 Fg^{-1} at 1 Ag^{-1} and cycle life over 1000 cycles. Moreover, the suggested method could be a suitable approach for the synthesis of other metal sulfides with graphene and graphene oxide [68].

Xia Wang et al. [2016] reported Ni-Co sulfide nanocomposite by single-step solvothermal method on graphene by employing polymers as an additive for the fabrication of Ni-Co-S@G, which can be utilized in supercapacitors. The prepared material electrode exhibit capacitance 1021 Fg^{-1} at 20 Ag^{-1}. and show high value of capacitance retention of 92.1% after 5000 cycles at 10 A g^{-1}. The reason for its excellent performance is its unique integrated nanostructure which also offers more electroactive sites results in high conductivity.

Moreover, in case of supercapacitor of Ni-Co-S@G//reduced graphene composites depict high value of 39.5 $Whkg^{-1}$ at power density of 1778 Wkg^{-1} power density

and it also shows outstanding cycle stability with the value of 84.4% capacitance retention over 15000 cycles [69].

Zhong-Shuai Wu et al. [2017] reported the synthesis of S-doped graphene fabrication for supercapacitors. The fabricated solid-state films depict a highly stable capacitance behavior which has the capacitance of 582 F cm^{-3} and showed outstanding rate capability with a capacitance value of 8.1 F cm-3 even at 2000 V/s, and depicts power density of 1191 W cm-3 [70].

Bingqiao Xie et al. [2015] reported the synthesis of MoS_2/N-doped graphene by one-pot hydrothermal method. Flower shaped MoS2/G was obtained with 3.5% nitrogen content on the graphene layers. Electrochemical measurements show the maximum specific capacitance of MoS2/NG electrodes with a value of upto 245 F/g. Furthermore, electrodes exhibit excellent cyclic stability with a value of 91.3% retention of capacitance over 1000 cycles. The synergistic effect gives an excellent performance of the MoS2/G hybrid [71].

Zhicai Xing et al. [2013] reported the nickel sulfides/reduced graphene oxide assisted with amino acids which act as reducing agents and donors of sulfur. The prepared nickel sulfides/rGO used as electrode materials for supercapacitors. Ultrafine particles of nanospheres lead to textural pores and the resulting material was found to have a capacitance of 1169 F/g at 5 A/g with excellent cycle life as well [72].

Juan Yang et al. [2015] reported a simple strategy for the fabrication of Ni-Co-S, which are deposited on graphene frameworks to form Ni-Co-S/G composites through a chemically converted method. Ni-Co-S depicts very high electrochemical activity. Ni-Co-S/G depicts capacitance value of 1492 F/g at 1 A/g, excellent rate capability of 96% with the increase in current density upto 50 A/g and also showed electrochemical stability excellently. A supercapacitor was formulated with Ni-Co-S/G hybrids as an electrode which depicts an energy density value of 43.3 Wh/kg and 0.8 kW/kg power density [73]. X. Yu et al. [2016] reported the incorporation of sulfur and phosphorus into three-dimensional highly porous graphene for enhancement of performance of supercapacitors. The 3D porous continuity is

preserved despite high loading amount of P and S of 4.6 and 5.8 % respectively. The composites depict a specific capacitance value of 438 F/g at a scan rate of 10 mV/s. Furthermore, at 500 mV/s specific capacitance value was 381 F/g which indicates the retention of 87.2 %. The capacitance retention of 93.4% was observed after 10000 charge/discharge cycles at 1 A/g. [74].

Haiming Zhang et al. [2013] described an approach for the development of reduced GO/Ni3S2 networks. The reduced graphene oxide/Ni3S2 nanoparticles were directly deposited onto the substrate by using an electrostatic spray. The results demonstrate a capacitance value of about 1424 F/g and a current density value of 75 A/g. The results showed that this material is a promising material for supercapacitors [75].

Parma Banerjee et al. [2015] stated the synthesis of composites of Ni-doped MOF with rGO. The crystals of MOF distribute over rGO. Nickel in Ni doped metal organic framework is found to involve in an efficient, reversible, redox reaction that shuffling from Ni(OH)2 to Ni in KOH electrolyte. Introduction of rGO to the composite develop synergy which increases the capacitance value dramatically upto 758 F/gm in the case of rGO-Ni-doped MOF composites in contrast to parent MOF which could only store 100 F/gm [76].

Xiehong Cao et al. [2015] described a convenient method for the fabrication of rGO composites with MoO3. The obtained material of rGO/MoO3 was further used in the application of supercapacitor and it exhibits outstanding electrochemical and mechanical stabilities. The wrapping around MoO3 with rGO sheets not only prevents the accumulation of MoO3 but also provides electrically conductive networks for electron transport. Therefore, their synthesized rGO/MoO3 composite exhibit outstanding rate capability and high cyclic stability in the case of supercapacitors. This novel strategy can also be implied on another graphene/metal oxide composites by a selection of appropriate MOFs [77]. Xiehong Cao et al. [2015] reported a convenient method for the synthesis of reduced graphene oxide which wrapped MoO_3 composites by using metal-organic framework. The obtained material of rGO/MoO_3 was further used in the application of supercapacitor and

it exhibit outstanding electrochemical and mechanical stabilities. The wrapping around MoO3but also provide electrically conductive networks for electron transport. Therefore, their synthesized rGO/MoO3 composite exhibit outstanding rate capability and high cyclic stability in case of supercapacitors. This novel strategy can also be implied on other graphene/metal oxide composites by selection of appropriate MOFs [77].

Dongying Fu et al. [2016] reported successful synthesis of metal organic framework-graphene oxide hybrids decorated on carbon nanotubes films (CNT) and furthermore to develop flexible porous and conductive electrode, deposition of polymer was made to develop polymer based hybrid which showed outstanding electrochemical activity. It showed a capacitance value of 128 $mFcm^{-2}$ observed by electrochemical measurements which is higher than that of CNT only in a 3 electrode system which indicates the positive impact of the addition of graphene which enhances the capacitance. They also perform an asymmetric study and observed that assembled optimum flexible supercapacitor depicts a capacitance value of 37.8 $mFcm^{-2}$ at 5mV/s and the energy density of this device was observed to be 0.051 $mWhcm^{-3}$ and volumetric power density was observed as 2.1 $mWcm^{-3}$ at a current density of 0.4 $mAcm^{-2}$. The fabricated device shows outstanding electrochemical and mechanical characteristics [78].

Pattarachai Srimuk et al. [2015] reported a composite of rGO/copper oxide MOF. The composite of rGO- copper oxide was fabricated by an ultra-sonication mixing of copper oxide and rGO. A simple spray coating technique was used to fabricate the supercapacitor electrode material of 10 wt% rGO composite exhibits a capacitance value of 385 F/g at 1A/g [79].

Lan wang et al. [2016] reported porous carbon composites by using graphene nanosheets and Zn MOF derived porous carbon film. The porous carbon obtained has a capacitance value of 345 F/g at a scan rate of 2 mV/s and retention of 99% capacitance over 10,000 cycles.Moreover, it can provide an energy density value of 30.3 Wh/kg and a power density of 137 W/kg [80]. Dennis Sheberla et al. [2016] reported electrochemical double layer capacitors (EDLCs) with high performance

as compared to batteries. MOF based device showed capacitance retention of 90% after 10,000 cycles [81].

Raul Diaz et.al [2011] reported various MOFs which show better electrical conductivities at 200 mVs^1 in an electrolyte which is composed of 0.1 M basic solution. Electrostatic forces are acting as dominant charge storage mechanism in case of this electrolyte while electrochemical efficiency is determined by different types of MOF [82].

Yan Yan et al. [2016] reported the successful synthesis of nickel oxide/ carbon based materials for supercapacitor applications. Nickel oxide/ carbon composite showed a capacitance value of 988 and 823 Fg^{-1} meanwhile with capacitance retention of 96.5% over 5000 cycles. This nickel oxide and activated carbons based material for supercapacitor showed capacitance of 230 230 $mFcm^{-2}$. with capacitance retention value of 92.8% after 5000 cycles. Energy density achieved is 4.18 $mWhcm^{-3}$ and maximum power density is reported to a value of 231.2 $mWcm^{-2}$ for the supercapacitor device [83].

2.2 Gap Analysis and Problem Statement

Table 2.1 gives a summarized analysis of the literature discussed in the previous section. This literature analysis leads to the areas where there is still room for improvement. Like better electronic conductivity [84][85[87][90], stretched cyclic lifetime, mechanical and chemical stability. The electrode materials in EDLC (as discussed earlier) are typically carbon-based materials due to their astonishing electrical conductivity, high surface area, low density, and high storage capacity.

It is observed that the supercapacitor's capacitance and charge storage depend on materials that are applied for electrodes. Therefore, the best method to solve the problem is to develop new materials with better capability in contrast to the existing electrode materials. The supercapacitor capacitance is greatly affected by the surface area of electrode materials.

Table 2.1: Comparison of Literature Reported Materials for Supercapacitor

Sr.No	**Authors**	**Materials**	**Capacitance (F/g)**	**Ref.**
1.	Yan et al.	Porous carbon derived from MOF-5	232	[54]
2.	Hau et al.	NiO based materials	116	[55]
3.	Purkaitet al.	reduced graphene oxide (rGO) networks on copper	81	[56]
4.	Liu et al.	SnO_2/Fe_2O_3 nanoparticles on graphene	165	[84]
5.	Hamid et al.	nickel sulfide wrapped with graphene	1000	[60]
6.	Liu et al.	(Co,Fe) transition metal sulfides	310	[63]
7.	Ramachandran et al.	ZnS/Graphene	197	[65]
8.	Cai et al.	GF/$NiCo2S_4$/Graphene	388	[66]
9.	Wang et al.	(NiS/GO) nanocomposites	800	[68]
10.	Wang et al.	Nickel Cobalt Sulphide/Graphene	1021	[69]
11.	Wu et al.	Sulphur/Graphene thin film	582	[70]
12.	Xie et al.	$MoS_2/Graphene$	245	[71]
13.	Xing et al.	nickel sulfides/rGO	761	[72]
14.	Yang et al.	Nickel/Cobalt Sulphide/Graphene	1492	[73]
15.	Yu et al.	N/P doped Graphene	438	[74]
16.	Zhang et al.	reduced graphene oxide/Ni_3S_2	406	[75]
17.	Banerjee et al.	rGO-Ni-doped MOF	758	[76]
18.	Fu et al.	FeMOF/GO/Carbon nanotube	128	[78]
19.	Srimuk et al.	Cu oxide/rGO	385	[79]
20.	Wang et al.	Zn MOF derived porous carbon film	345	[80]
21.	Yan et al.	Ni Oxide/Carbon	988	[83]

In various metal composites and carbon electrode materials, the effects of crystal structure, morphology, doping and microstructure on their electrochemical performance in different electrolytes are still poorly investigated and understood. This research aims to study composites of reduced graphene oxide with MOF material to fulfill this research gap by enhancing electrochemical performance. The major problems of supercapacitor are high cost, low energy density, upgrading of current technologies is desired to develop graphene based electrode material that delivers improved morphology at low cost, electrode preparation method which can hold the porous structure and electrical properties of the electrode.

2.3 Proposed Research Methodology

To develop high performing and stable graphene based electrode materials, three different metals namely nickel, copper and cobalt were proposed. These metals are incorporated in graphene in the form of their metal organic framework which also has a highly active surface area. The three metals selected are low-cost transition metals. To begin with, the proposed plan was to oxidize graphite powered to graphene oxide(GO). In a further step, the GO is converted into its reduced form rGO. Further composites of 5wt% rGO with MOFs of nickel, copper and cobalt are proposed. The layout of the proposed plan for the synthesis of electrode material is given in figure 2.1

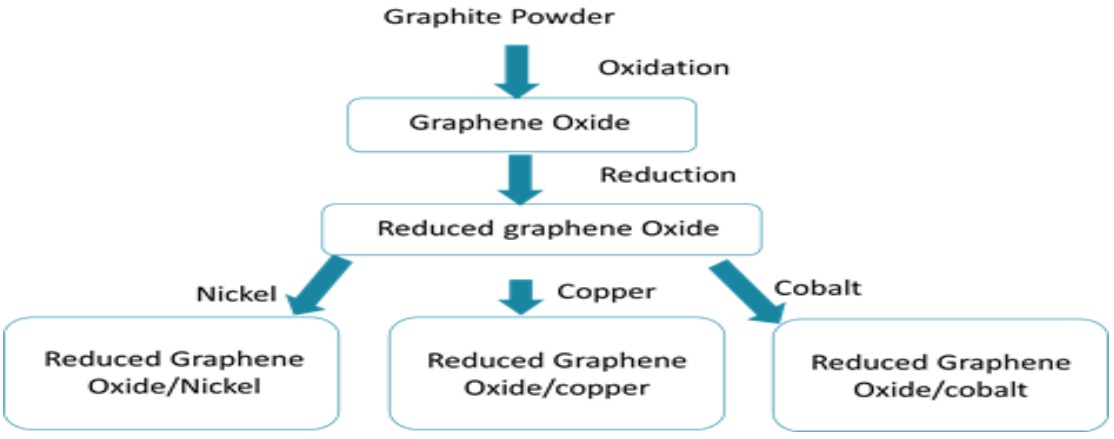

FIGURE 2.1: Proposed Synthesis Methodology of Graphene Based Electrode Materials with three Different Metals.

In the next step, three different techniques are proposed to study the physical and chemical characteristics of prepared materials. In which X-Rays Diffraction (XRD) was aimed to study the structural properties of composites, whereas Scanning Electron Microscopy (SEM) is employed to study the morphology of the graphene based composite materials. Fourier Transform Infrared Spectroscopy (FTIR) is proposed to investigate the different types of bonds present in graphene and its composites. The outline of characterization techniques is given in figure 2.2.

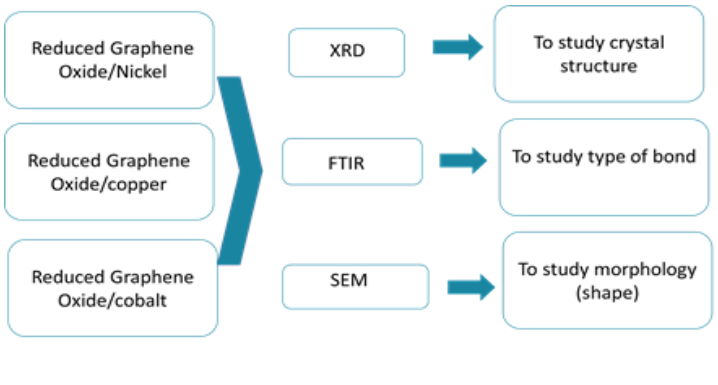

FIGURE 2.2: Proposed characterization technique to explore the physical and chemical properties of materials

To investigate the electrochemical performance for supercapacitor applications the materials are proposed to be tested using Potentiostat. Three major parameters focused to investigate are cyclic voltammetry (CV) to determine capacitance, Galvanostatic Charge/Discharge Cycle (GCD) to measure charge/discharge properties and Eelectrochemical Impedance Spectroscopy (EIS) to measure resistance. The outline of electrochemical performance study is given in figure 2.3.

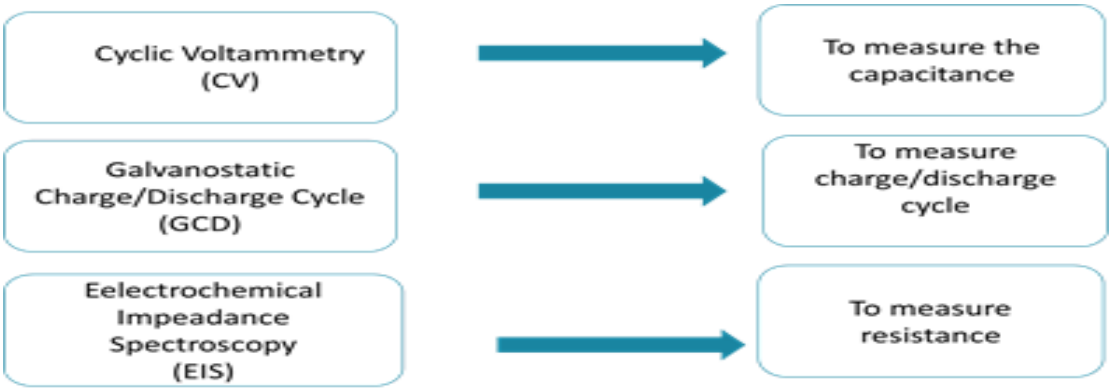

FIGURE 2.3: Outline of Proposed Plan to Investigate the Electrochemical Performance of Supercapacitor Electrode Materials

2.4 Research Contribution

The present research work is focused to develop the graphene base electrode materials and studying their performance for supercapacitors applications. Reduced graphene oxide is modified by making its composites with three different transition metals namely nickel, copper and cobalt in the form of their metal organic framework. The materials are characterized by SEM, XRD, EDX and FTIR to investigate different physical and chemical properties. The conductive nature of graphene oxide decorated with metals shows enhancement in the electrochemical properties and provides a promising candidate for supercapacitors base on low-cost transition metals incorporation.

Chapter 3

Synthesis of Graphene Based Electrode Materials

The third chapter focuses on the synthetic approach used to synthesize graphene based materials. The first section 3.1 gives details about graphene oxide synthesis by using reported Hummer's method. In the second section 3.2, the fabrication of rGO from GO by reduction method is elaborated. In the third section 3.3 preparation of rGO based composites with copper is outlined, section 3.4represents rGO/ nickel composite synthesis 3.5 presents rGO/cobalt composite synthesis by solvothermal approach.

3.1 Synthesis of GO

Synthesis of graphene oxide (GO) was executed according to well-known Hummer's method. The whole method was alienated into three segments to follow temperature requirements. In the first phase graphite (4g) and $NaNO_3$ (4g) were dissolved in 100 ml sulphuric acid and stirred for about 2 hours at $5°C$ in an ice bath to get a homogenous mixture. In the second phase, the ice bath was removed, the temperature was maintained at $35 \pm 3°C$ and potassium permanganate (12g)

was gradually mixed to the above mixture and stirred for 48 hours to ensure complete oxidation. A thick green paste was attained after 2 days of stirring. In third phase, in order to dilute green paste, deionized water (200 ml) was slowly added to avoid rise in temperature and splashing. Furthermore, hydrogen peroxide (10ml) was added to complete oxidation and stirred for the next 30 minutes. Finally, the product was yellowish brown. The product was repeatedly washed through centrifugation at 8000 rpm for 30 minutes with dilute HCl and water till pH 6-7 pH was achieved followed by vacuum drying at $50°C$ overnight [86, 87].

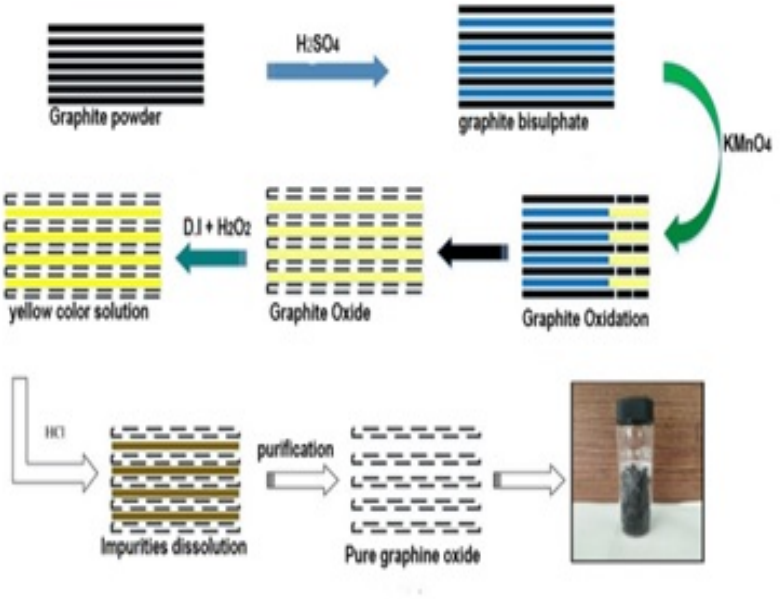

FIGURE 3.1: Synthesis of Graphene Oxide by Hummer's Method.

3.2 Synthesis of rGO

Reduced graphene oxide was fabricated from graphene oxide by the reflux method. Graphene oxide (100 mg) was sonicated in deionized water (100ml) for one hour to obtain a brown aqueous suspension.

Above suspension along with hydrazine hydrate (1ml) was poured into the round bottom flask and refluxed for 24 hours at $100°C$ an oil bath. Black, porous and hydrophobic material was gradually collected on the surface of an aqueous solution.

Product was collected through filtration membrane under vacuum, washed with ethanol and water with subsequent vacuum drying $60°C$ [88].

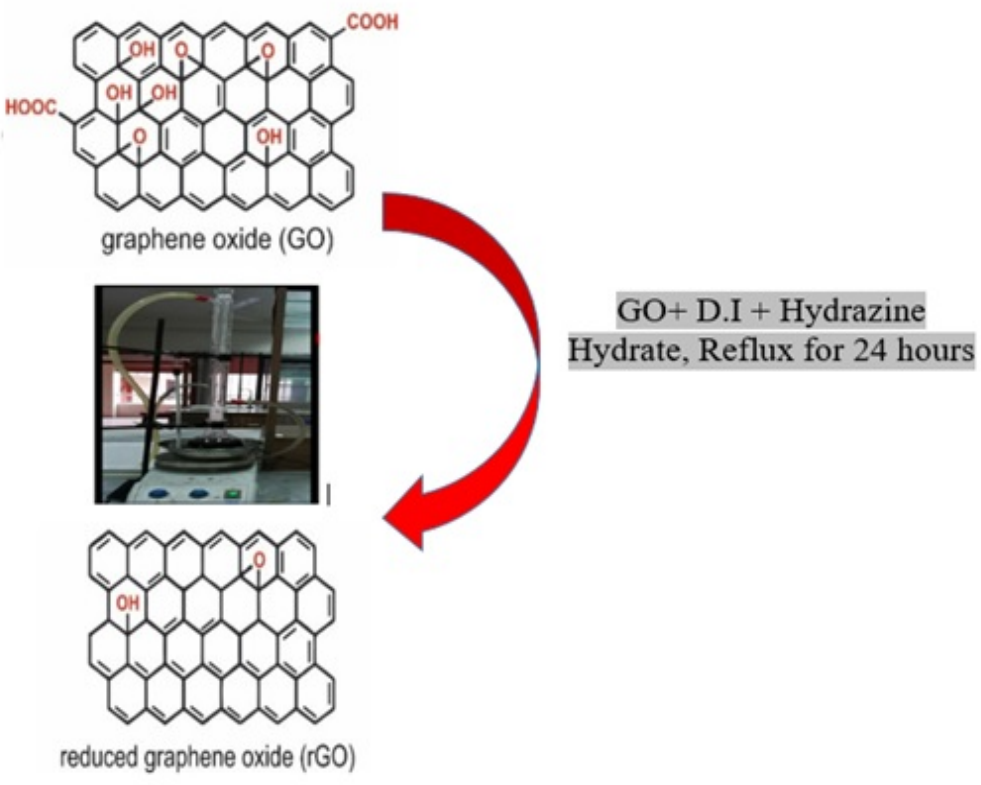

FIGURE 3.2: Synthesis of Reduced Graphene Oxide by Reflux Method

3.3 Synthesis of Reduced Graphene Oxide/Copper

In the synthesis of Cu BTC/ 5wt % rGO composite, BTC (1.5 g) was dissolved in DMF/C_2H_5OH solvent mixture (45 ml) while on the other hand metal salt solution was prepared by dissolving copper nitrate (3.114g) in deionized water. Both solutions were mixed together by stirring followed by the addition of 23 mg graphene oxide. After stirring the final mixture was shifted to the high-pressure autoclave with Teflon cavity and put in the oven for reaction at $100°C$ for 12 hours. The product was thoroughly washed with ethanol and methanol with subsequent vacuum drying at $60°C$ for 10 hours [89].

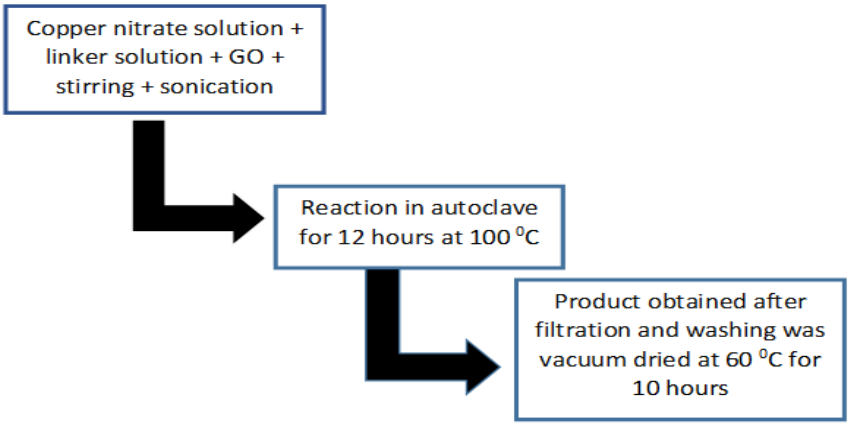

FIGURE 3.3: Solvothermal Synthesis of Reduced Graphene Oxide/Copper

3.4 Synthesis of Reduced Graphene Oxide/Nickel

In the synthesis of Ni BTC/ 5 wt % rGO composite, the first linker solution was prepared by dissolving BTC (1 g) in DMF/C_2H_5OH solvent mixture 34 ml. Metal salt solution prepared by mixing nickel nitrate (2 g) in 17 ml deionized water was poured into linker solution followed by stirring to get a homogenous mixture. An appropriate amount of rGO (15 mg) was thoroughly dispersed into above solution via sonication. After 2 hours the sonication reaction mixture was shifted in an autoclave for reaction in the oven at $120°C$ for 24 hours. After filtration and washing of product with ethanol/ water repeatedly was vacuum dried at $50°C$ for 24 hours [90].

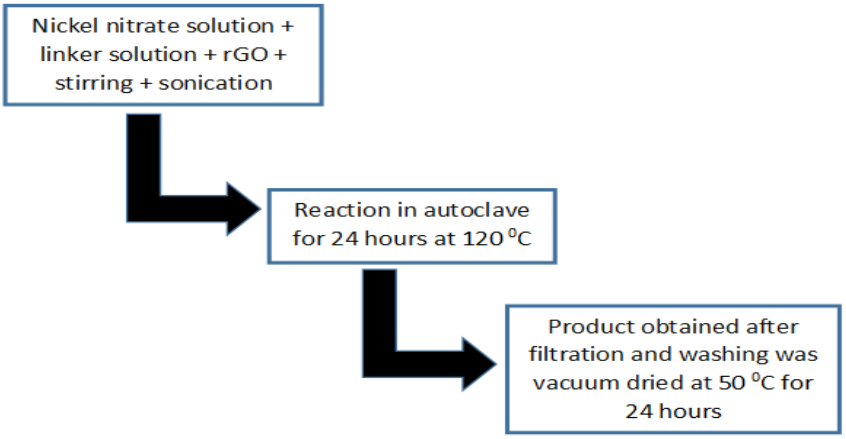

FIGURE 3.4: Solvothermal Synthesis of Reduced Graphene Oxide/Nickel

3.5 Synthesis of Reduced Graphene Oxide/Cobalt

Co BTC/ 5 wt % rGO composite was synthesized by the reported method. (1g) Benzene tricarboxylic acid (BTC) was dissolved in DMF/C_2H_5OH mixture (1:1) while cobalt nitrate solution was prepared by stirring (2 g) nickel nitrate in deionized water (17 ml). After triethylene amine addition into inker solution it was slowly poured into metal salt solution with 30 minutes stirring to acquire homogenous mixture. A suitable amount of rGO (0.15g) was carefully dispersed into above mentioned solution by sonication. After two hours of sonication resultant mixture was moved to the autoclave for 24 hours reaction in an oven at $100°C$ hours overnight. The product achieved after reaction finalization was repeatedly washed with ethanol and then with water followed by vacuum drying at $50°C$ overnight to get dried product [91].

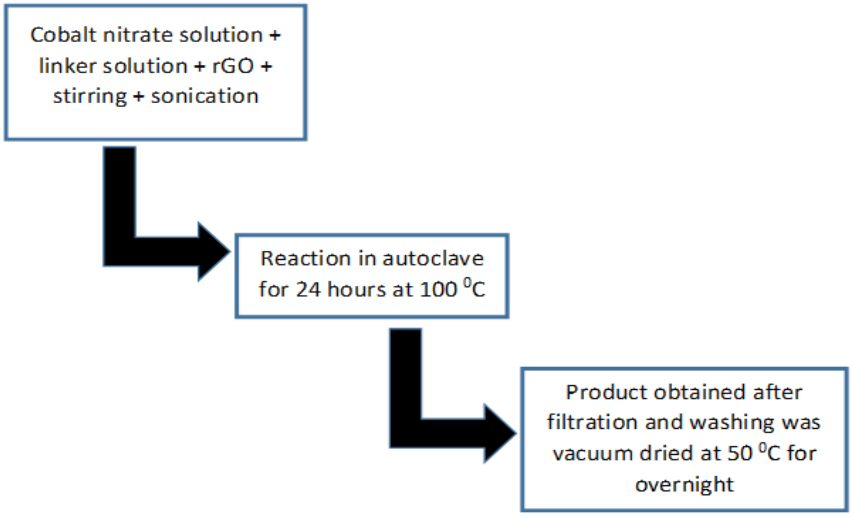

FIGURE 3.5: Solvothermal Synthesis of Reduced Graphene Oxide/Cobalt

Chapter 4

Characterization of Prepared Materials

In this chapter, the first Section 4.1 discusses the general overview of various characterization techniques used to explore the physical and chemical properties of electrode materials. In the second section 4.2, the details about the determination of crystal structure of prepared material via XRD technique are discussed. The next section of this chapter 4.3 presents a detailed FTIR spectrophotometer analysis of functional groups present in synthesized electrode materials. In the last section 4.4, characterization of prepared material with respect to surface structure and morphology is presented by using scanning electron microscopy.

4.1 Characterization

To determine crystal structure, X-ray Diffraction (XRD) measurements are carried out by X-ray powder diffractometer (Bruker D8, Germany) coupled with Cu Kα at $\lambda = 1.5418 \ \ A^{\circ}$ within 2 theta range of $5 - 80^{\circ}$ was at step size 4 s^{-1} . Surface structure and morphology are analyzed by scanning electron microscopy (VEGA3 TESCAN) at voltage 20 KV. Agilent FTIR spectrophotometer is used to check the occurrence of functional groups in synthesized compounds.

4.2 X-Ray Diffraction

The crystal structure of the prepared materials shown by powdered XRD (Figure 4.1.

4.2.1 Nickel-Based Composite

The sharp peaks show the crystallinity of prepared composites. Peaks at 23°(004) and 17°(002) are attributed to the rGO and incomplete reduction of the GO peak, this peak is increased by 5 wt%. These peaks are not substantial in other prepared samples. This may be due to the coinciding of substantial peaks due to metal's crystalline nature. Also, this indicates that rGO did not affect the metal and ligand interactions. Peaks at 24.5°(600) are due to formation of metal oxides and hydroxide. Peaks at 2θ values of 35°(022), 42°(512), and 51°(226) show the occurrence of Ni.

4.2.2 Cobalt-Based Composite

For Co based composite material, sharp peaks in XRD show the crystalline nature of the prepared composites. The occurrence of rGO in samples was established by a peak at 23° but sharp peaks of metal in same region overlap the rGO peak and give a hint about the noninterference nature of rGO. Metal oxides and hydro-oxide formation is shown by peaks at 2θ value $18°, 31°, 32°, 38°, 45°, 51°, 56°, 60°, 68°, 78°$ while the Co occurrence was shown by peaks at $28°, 34°$, and 53°. The peak at 2θ value 43° relates to metallic cobalt (JCPDS cards #15–0806).

4.2.3 Copper-Based Composite

The presence of distinctive peaks at 2θ values of 6.56, 9.32, 11.2, 13.28, and 18.92 are (200), (220), (222), (400), and (440) correspondingly signify the crystalline nature of MOF. The particularly strong peak at (222) points out that the preference

of crystals alignment is out of the plane (222).

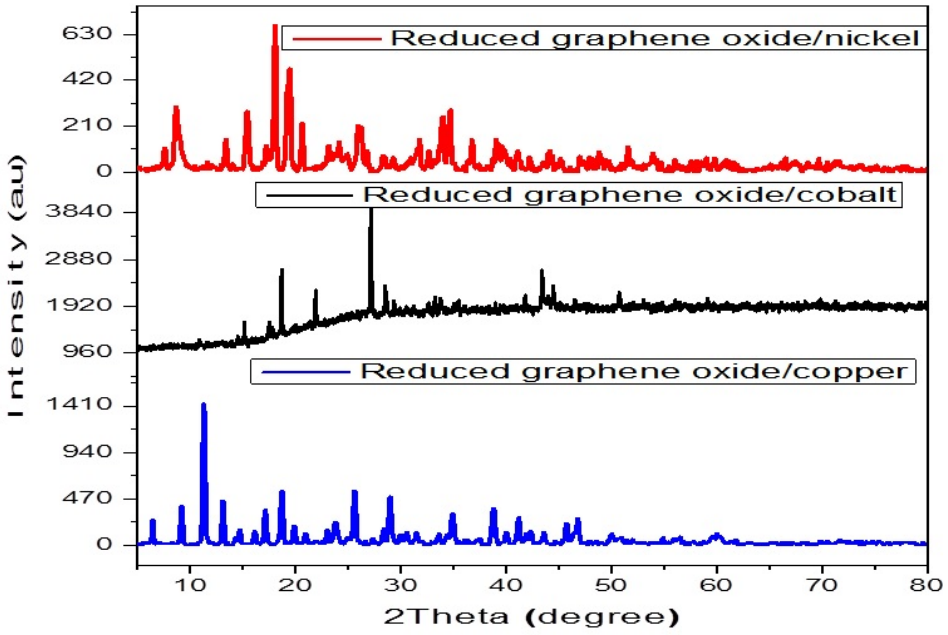

FIGURE 4.1: XRD Analysis of Reduced Graphene Oxide/Nickel, Reduced Graphene Oxide/Cobalt and Reduced Graphene Oxide/Copper

4.3 Fourier Transform Infrared Spectroscopy

FTIR is an expedient method to conclude the functional group's existence in the synthesized compound. The broad peak amid 3500 and 3200 cm^{-1} is an evidence of OH on the exterior side as well as hydrogen bonded water molecule between metal-BTC units while 1626 cm^{-1} peak manifests the C=C of aromatic cycle. The peak due to C–O–C of epoxide group of GO give at 1224 cm^{-1}. The peak at 1373 cm^{-1} peak indicates C-O while C=O peak appears at 1644 cm^{-1}. The peak at position 1477 cm^{-1} further verify the OH group existence [92]. The peak at position 730 cm^{-1} is a clear indication of linking of Copper with oxygen of COOH group.

The existence of functional groups was confirmed through FTIR Figure 4.2. The presence of surface adsorbed water was indicated by a wide-range adsorption band

of 3600–3000 $cm^1$to OH group stretching vibrations [93, 94]. The shift in C=O peak from 1715 to 1608 as well as no peak in the region of 1800-1600 ensure COOH group deprotonation, further approved by Ni-O peak at 726 cm^{-1} [95, 96]. The symmetric and asymmetric vibration peaks of carboxylic group are visible at 1350-1450 and $1550-1640$ cm^{-1} along with peaks due to C=C stretching mode between $1600-1400$ cm^{-1}. These bands also authenticate metal-ligand coordination and successful composite fabrication [97, 98].

The FTIR spectrum of Co BTC/5 wt % rGO composite is presented in Figure 4.2. The appearance of wide absorption in the range of $2900-3600$ cm^{-1} is due to physically adsorbed H_2O [93, 94]. Deprotonation of COOH group in presence of TEA and linker interaction with cobalt was portrayed by the band at 1608 cm^{-1} in place of 1715 cm^{-1} [96, 99]. Moreover, (C=C) aromatic and C-O stretching vibration band arise between1400-1600 and at 1373 cm^{-1} respectively. Co-O coherence and hybrid synthesis were certified by band present to 700 cm^{-1}. [97, 100, 101].

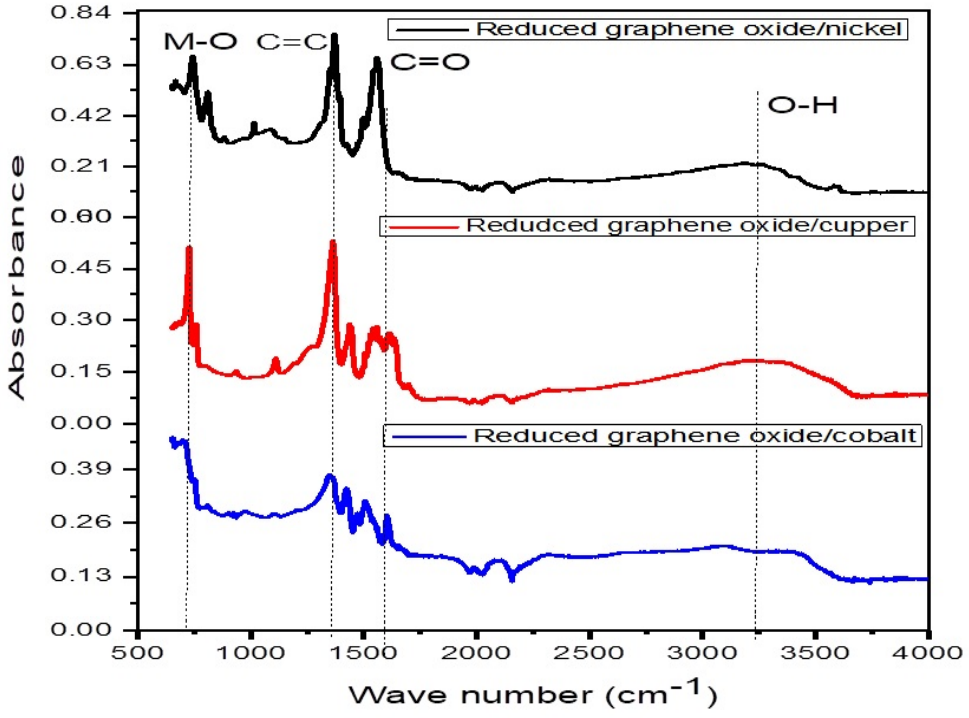

FIGURE 4.2: IR Analysis of Reduced Graphene Oxide/Nickel, Reduced Graphene Oxide/Cobalt and Reduced Graphene Oxide/Copper

4.4 Scanning Electron Microscopy and Electron Dispersive Spectroscopy

SEM images of prepared materials are shown below. Cobalt looks spherical, and the morphology of the prepared material is similar to the reported literature. Furthermore, particle accumulation decreases the crystallinity of the sample. Wrinkled structures of rGO in the material are noticeable.

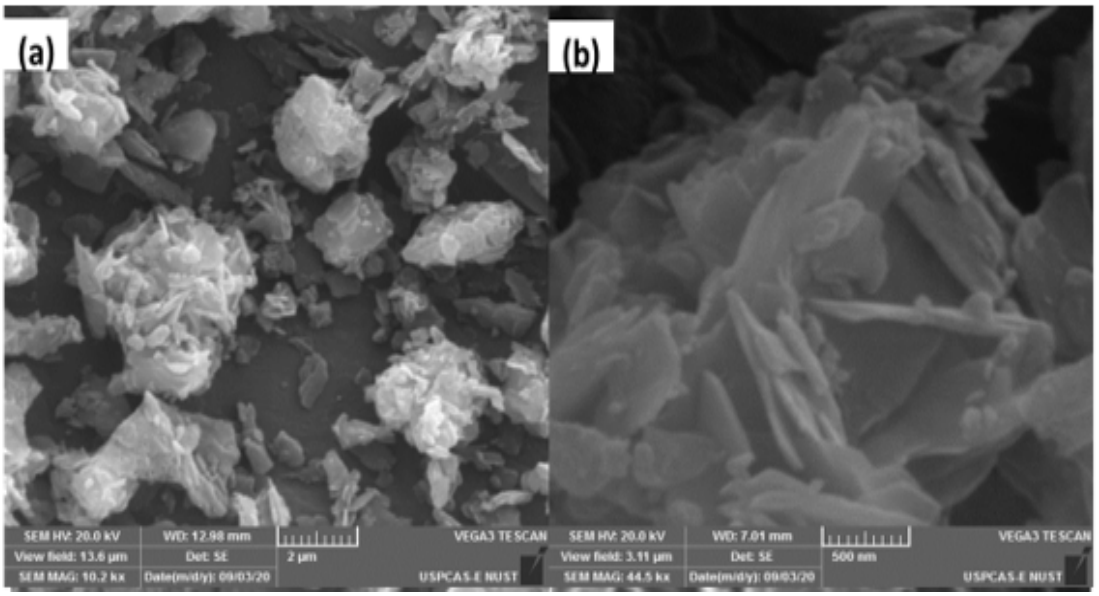

FIGURE 4.3: (a-b) SEM Analysis of rGO/nickel

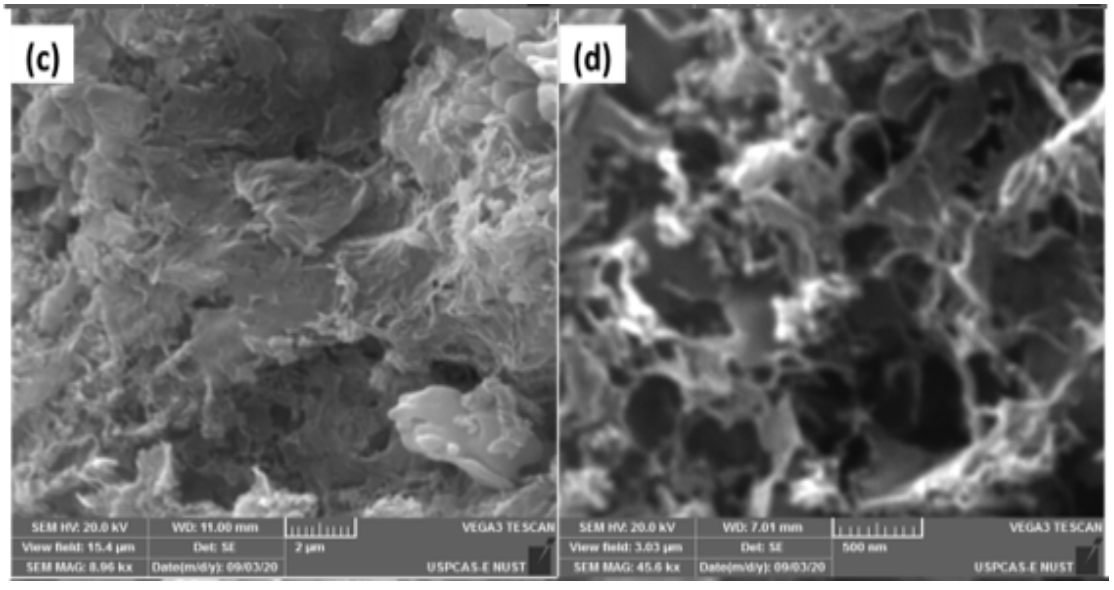

FIGURE 4.4: (c-d) SEM Analysis of rGO/Cobalt

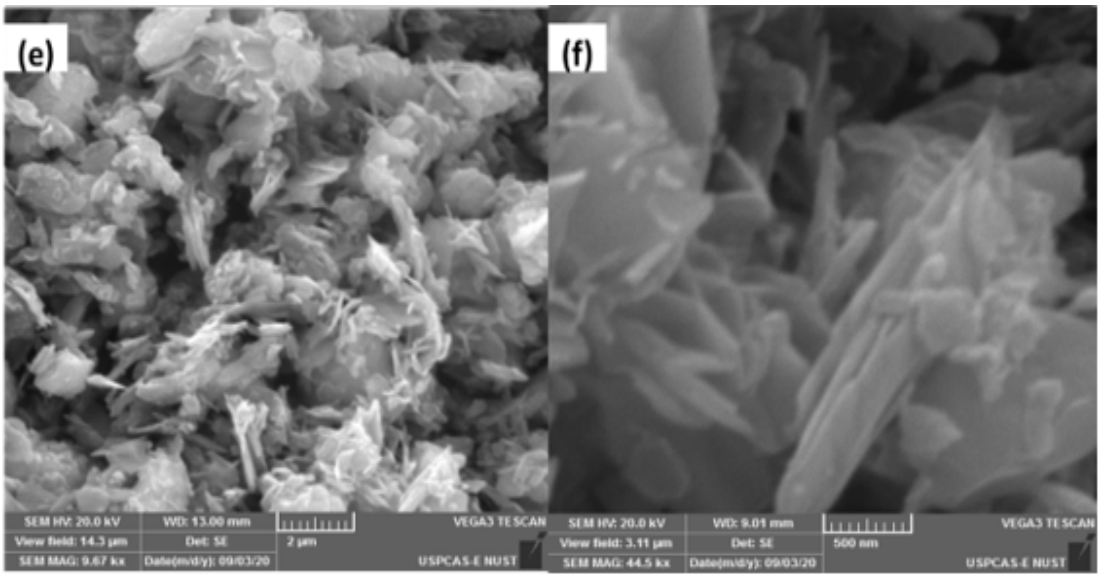

FIGURE 4.5: (e-f) SEM Analysis of rGo/Copper

For the case of copper-based samples, the morphology is wrinkled that is the typical characteristic of rGO. Many Cu based particles are evenly distributed on rGO. In addition, rGO/nickel SEM images confirm the synthesis of Ni-based BTC samples has almost plate shape and rGO flakes are observable in each composite. The relative wt % of metals, carbon and oxygen is validated via EDX analysis that is illustrated in Table 4.1. Following analysis confirms there is no other element presence except cobalt, nickel, copper, carbon and oxygen, thus confirms the absence of any other impurity present in prepared samples.

TABLE 4.1: Energy Dispersive X-rays (EDX) Analysis of Reduced Graphene oxide/nickel, Reduced Graphene Oxide/Cobalt and Reduced Graphene Oxide/-Copper

Samples	**Element**	**Wt%**	**At%**
Reduced Graphene Oxide/Cobalt	C	45.55	55.39
	O	46.80	4272
	Co	7.65	1.90
Reduced Graphene Oxide/Copper	C	57.01	71.75
	O	25.21	23.82
	Cu	17.74	4.44
Reduced Graphene Oxide/Nickel	C	40.31	51.22
	O	47.58	45.39
	Ni	12.11	3.4

Chapter 5

Electrochemical Analysis

In this chapter the electrochemical analysis of the prepared materials is discussed. The electrochemical properties are investigated by using various electrochemical methods such as cyclic voltammetry (CV), galvanostatic charge-discharge (GCD) and electrochemical impedance spectroscopy (EIS). In the first section 5.1, the CV studies of prepared material at varying scan rates are presented and subsequently, the capacitance and energy density of prepared materials are determined.

The second section 5.2 highlights result from chronopotentiometry method which is utilized to determine the charge-discharge performance during the electrochemical activity. The specific capacitance and energy are also calculated via GCD curves. In the third section 5.3, Electrochemical impedance spectroscopy (EIS) results are presented with respect to material Rct (charge transfer resistance), Rs (solution resistance) C_{dl} (double layer capacitance) and W_o (Warburg diffusion element).

5.1 Cyclic Voltammetry

The electrochemical performance of the prepared materials is accomplished on an electrochemical Workstation CHI 760E (CH Instrument, Texas, USA) with 3 electrode setup. Counter electrode of a platinum wire and Ag/AgCl (SC) reference electrode are employed.

To make the homogeneous ink for the working electrode (GC); 2mg of material was dispersed in 0.08 mL of ethanol solution and 0.02 mL of Nafion solution (5 wt. %) ultrasonically for 2-3 hours. The polished GCE (3 mm diameter) was coated by the suspension (1.5 μL).

The investigation of the electrochemical behavior of synthesized samples was performed via cyclic voltammetry (CV), galvanostatic charge-discharge (GCD) and electrochemical impedance spectroscopy (EIS) in an electrolyte of 2M KOH solution.

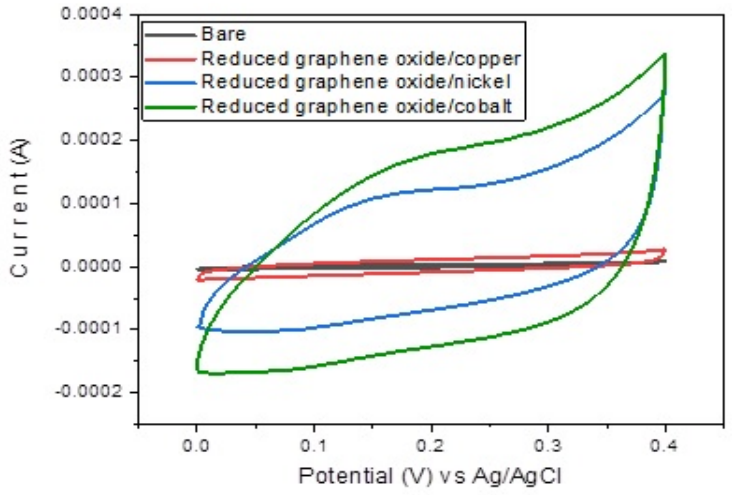

FIGURE 5.1: (a) Comparative CV curves at scan rate of 50mV/s

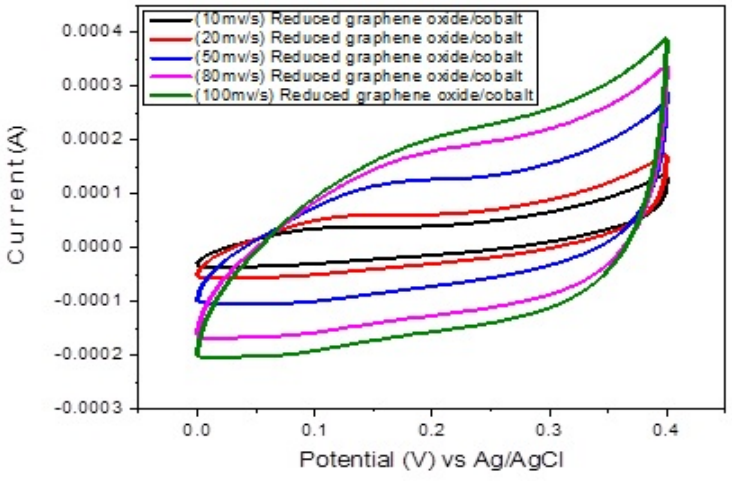

FIGURE 5.2: (b) CV curves of rGO/ cobalt

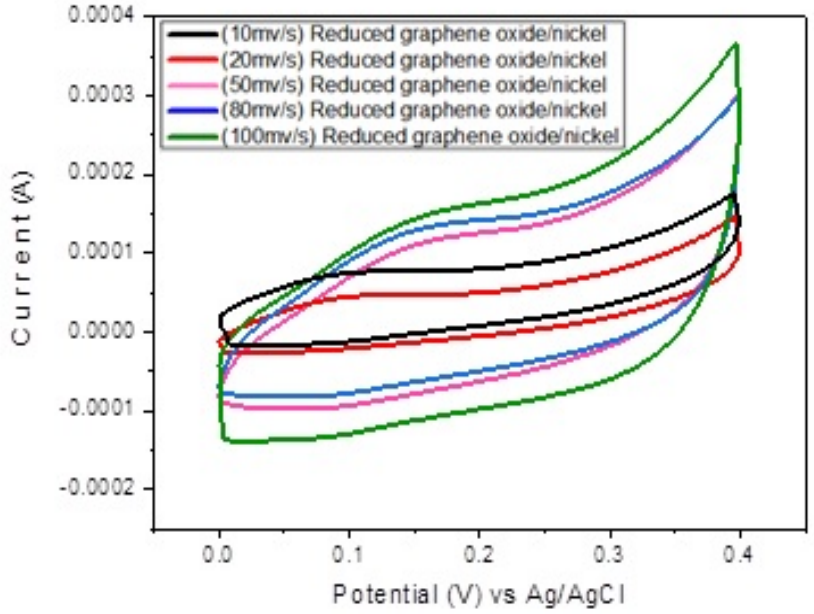

FIGURE 5.3: (c) CV curves of rGO/ nickel

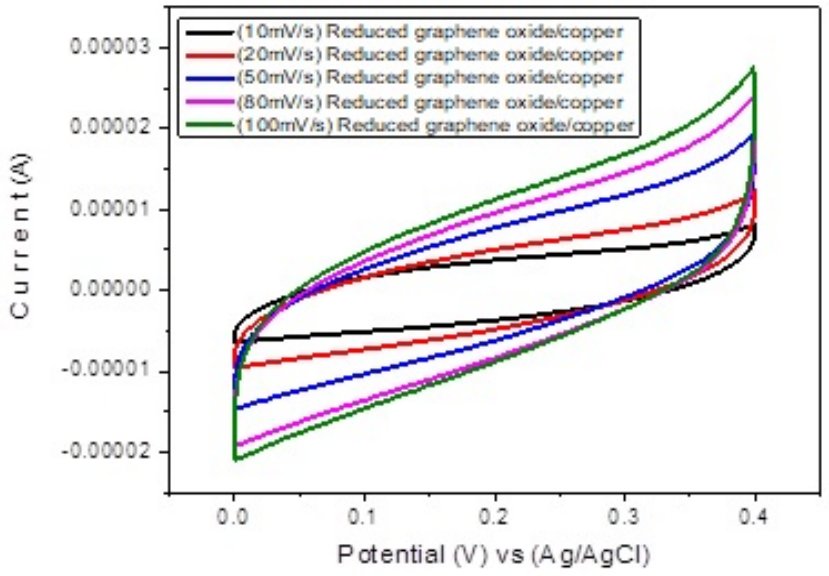

FIGURE 5.4: (d) CV curves of rGO/copper

Figure 5.1 (a) illustrated the comparative CV study of prepared materials, among all composites, reduced graphene oxide/cobalt show specific capacitance up to 562.12 F/g in contrast to other two samples like rGO/nickel and rGO/copper specific capacitance due to high total surface area and high current density values.

The CV curve high area exposes the ability of electrode for charge storage which is associated with the real active surface area [102]. The electrochemical demonstration of rGO/cobalt, rGO/nickel and rGO/copper by cyclic voltammetry was premeditated by applying scan rates variable from 10-100 mV/s as illustrated in Figure 5.2(b)-5.4 (d).

It was detected that via increasing the scan rates capacitance of prepared sample increases due to redox reaction of nanoporous material, at low scan rate outer and inner both parts exhibited these reactions while at high scan rate material outer part participate in redox reaction.

In CV curves two peaks appear i.e. anodic and cathodic peaks are interrelated to positive and negative current, correspondingly. In case of reduced graphene oxide/cobalt/nickel and copper capacitance characteristics are mainly directed via Faradaic redox reaction of cobalt, nickel and copper cation[103] and attributed to the redox reactions of $Co^{2+}/Co^{3+}/Co^{4+}$ Cu^{2+}/Cu^{3+} and Ni^{2+}/Ni^{3+}[104].

The values of specific capacitance and energy density for reduced graphene/cobalt, reduced graphene/nickel and reduced graphene/copper is calculated by using the following expressions (given in **Table 5.1**). From cyclic voltammetry, the specific capacitance is calculated via the following [103].

$$C = A/2\Delta V m k \tag{5.1}$$

C = specific capacitance (F/g), A = average integral area under the curve, ΔV potential window (V), k = scan rate and m = mass loading of the active material in the working electrode (g). In addition, energy density is calculated via following equation [103].

$$E_g = \frac{1}{2} C_p \Delta V^2 \tag{5.2}$$

Where E_g is energy density (Wh/Kg), C_p = specific capacitance (F/g) and ΔV = potential window (V).

TABLE 5.1: The Specific Capacitance and Energy Density of Reduced Graphene/ Cobalt/Nickel and Copper

Sr.No	**Catalyst**	**KOH Conc (M)**	**Specific Capacitance (F/g)**	**Energy Density (Wh/Kg)**
1	Reduced graphene oxide/copper	2	60.92	4.87
2	Reduced graphene oxide/nickel	2	542.34	43.38
3	Reduced graphene oxide/cobalt	2	562.12	44.96

5.2 Galvanostatic Charge and Discharge Curves

The chronopotentiometry method is used to perform the charge-discharge curve in the potential window of 0.4 V at 0.01-0.05 mA cathodic current to get the discharge time. The galvanostatic charge and discharge (GCD) curves of the rGO/cobalt, rGO/nickel and rGO/copper at a range of different current densities having 0.0 to 0.4 V potential window are illustrated in Figure. 5.2. (a-d). The prepared rGO based composites exhibit hat-like shapes that also confirm the Faradic redox reactions happening[105, 106].

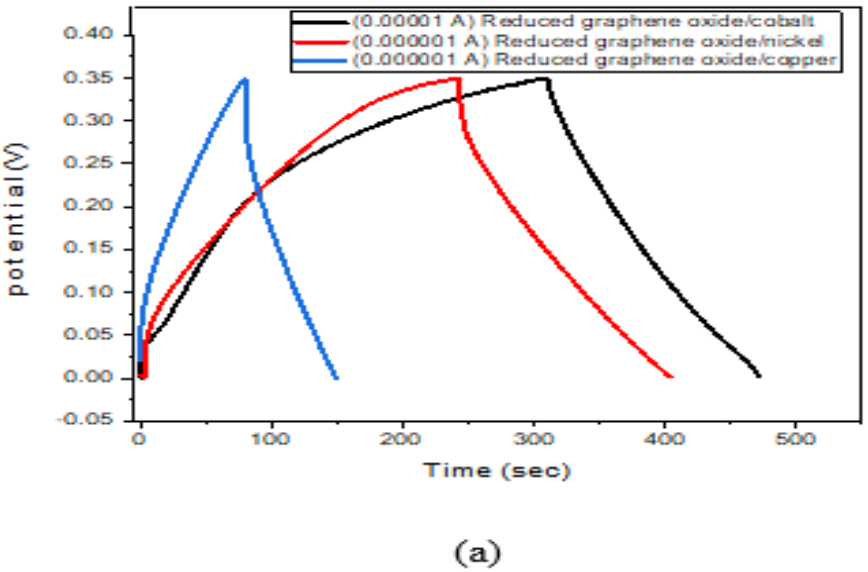

(a)

FIGURE 5.5: Comparative GCD curves at (0.01 mA)

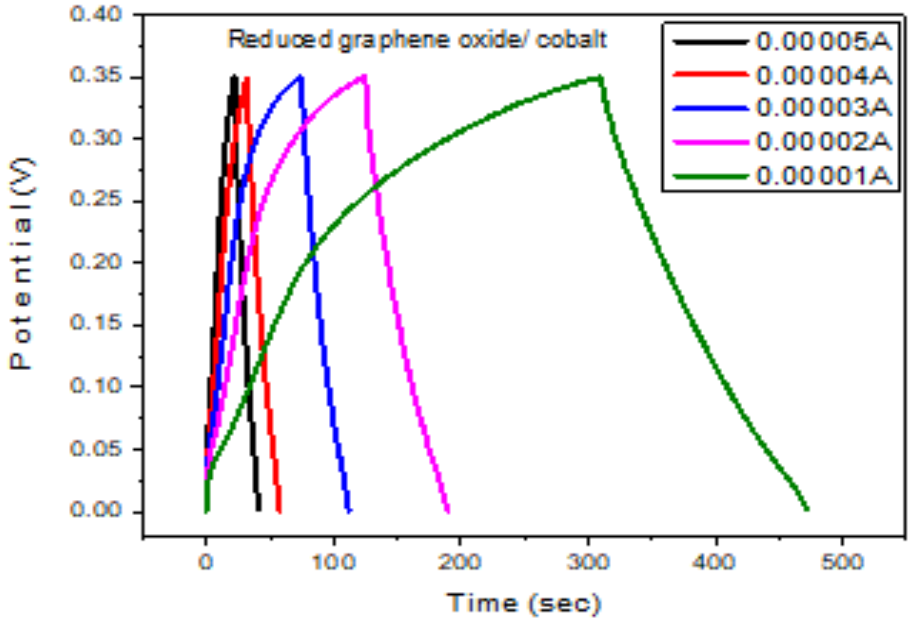

(b)

FIGURE 5.6: GCD of reduced graphene oxide/ cobalt

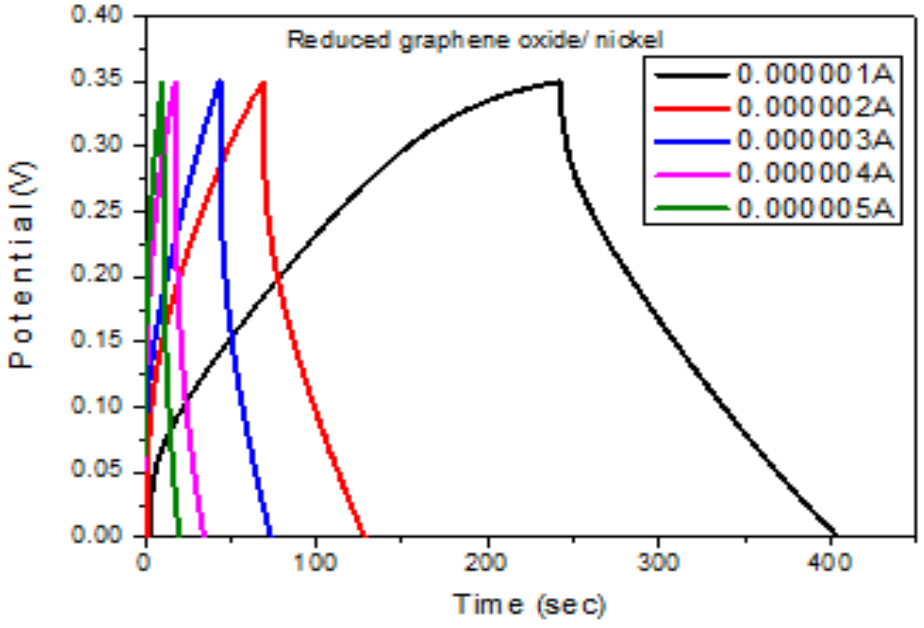

(c)

FIGURE 5.7: GCD of reduced graphene oxide/ nickel

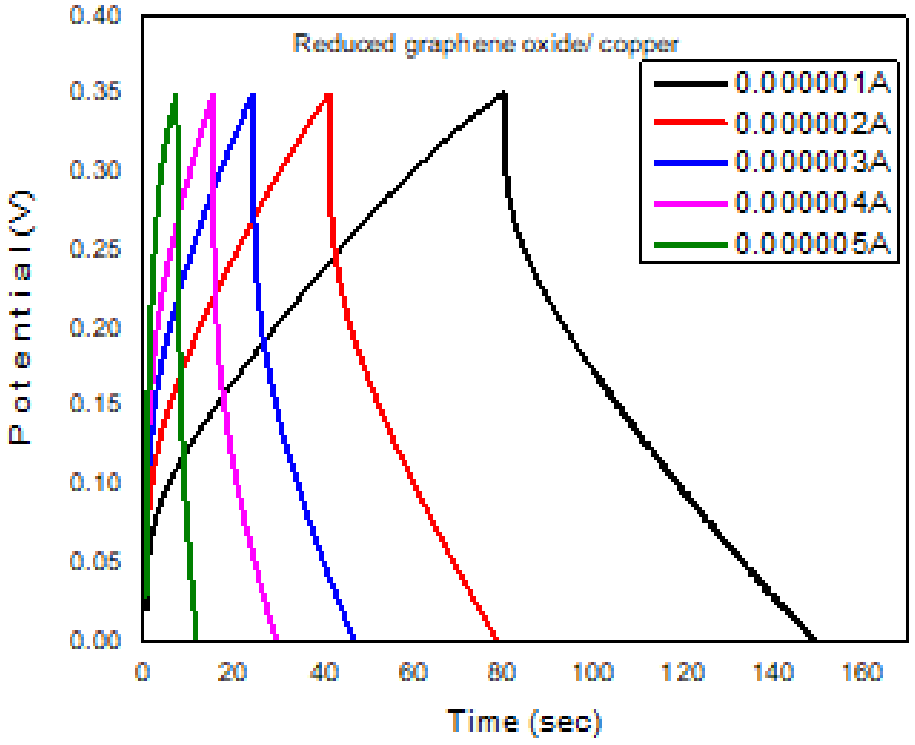

(d)

FIGURE 5.8: GCD of reduced graphene oxide/copper

The capacitance and energy density can be determined from GCD curves using the given relations (given in table 5.2).

$$Cp = I \times \Delta t / \Delta V \times m \tag{5.3}$$

Cp = specific capacitance, I = current, ΔV = potential window, Δt = time interval for voltage and m = mass of active material used. In addition, energy density is calculated via following equation. In addition, energy density is calculated via Equation 5.2.

In cyclic voltammetry, the time of the experiment is well distinct via the scan rate and potential window. In Galvanostatic studies, the charging-discharging currents and potential window are quantified with respect to the total time of the experiment in accordance with the cell capacitance.

Secondly, the average current is considered for calculating specific capacitance in the cyclic voltammogram method, while in the charge-discharge method, the charge-discharge current is constant and the difference in specific capacitance is measured.

TABLE 5.2: The Specific Capacitance and Energy Density Values Calculated From GCD Curves

Sr.No	**Catalyst**	**KOH Conc (M)**	**Specific Capacitance (F/g)**	**Energy Density (Wh/Kg)**
1	Reduced graphene oxide/copper	2	29	2.19
2	Reduced graphene oxide/nickel	2	94	7.47
3	Reduced graphene oxide/cobalt	2	204	16.26

5.3 Electrochemical Impedance Spectroscopy (EIS)

Electrochemical impedance spectroscopy (EIS) was accomplished to comprehend the kinetic behavior of ionic diffusion liable for electrode charge storage capability, employing a frequency range of 1 to 100 kHz in 2 M KOH electrolyte solution, conductivity and charge transfer resistance (R_{ct}) illustrated in Figure 5.9. In EIS spectrum it is observed that a small diameter arc exhibited by the prepared sample corresponds to lower resistance values, among all prepared composites rGO/ cobalt illustrated a lower value of (R_{ct}) (as given in Table 5.3) in contrast to the other two samples such as rGO/nickel and rGO/copper which is because of fast transfer of electron [104]. In addition, Nyquist plot matched well with an equivalent circuit as shown in figure 5.9, (to calculate the resistance values the following circuit for the simulation used as reported in the literature) and fitted data are given in Table 5.3. ESR is the equivalent series resistance representing the resistance for current collectors, electrode materials, electrolytes as well as contact resistance; whereas

the; (R_{ct}) is represents the resistance with respect to charge transfer. In addition to this double layer, capacitance is represented as W_o is the Warburg diffusion element.

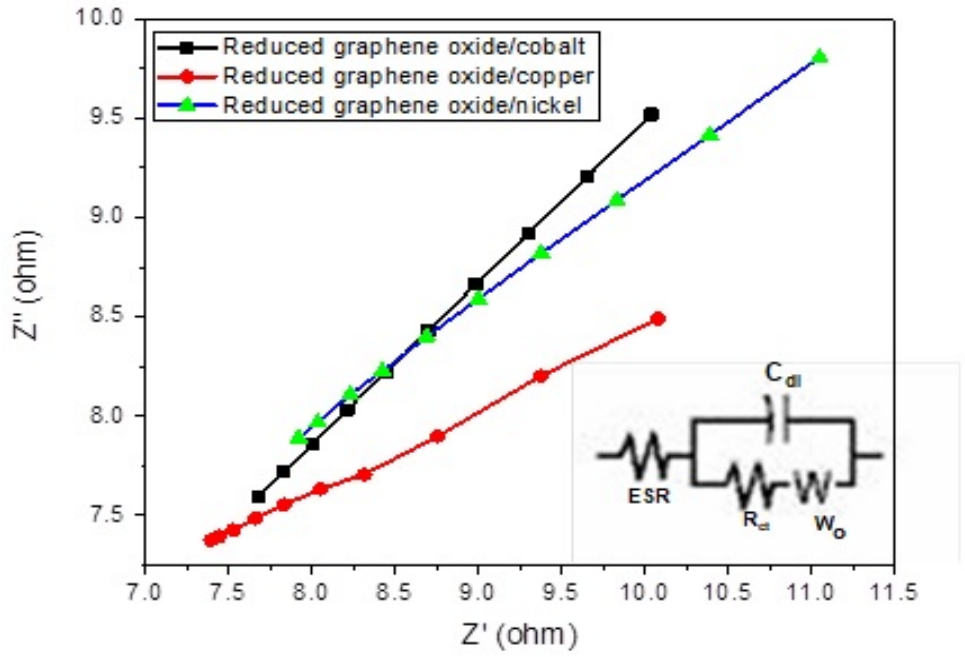

FIGURE 5.9: Comparison study of EIS for reduced graphene oxide/cobalt, reduced graphene oxide/nickel and reduced graphene oxide/copper in 2M KOH at 1-100kHz

TABLE 5.3: R_s, R_{ct} and C_{dl} of Reduced Graphene Oxide/Cobalt, Reduced Graphene Oxide/Nickel and Reduced Graphene Oxide/Copper

Electrode Material	$R_s(\Omega)$	$R_{ct}(\Omega)$	$C_{dl}(F/g)$	$W(\Omega S^{1/2})$
Reduced Graphene Oxide/Copper	7.254	46.97	$6.32e^{-7}$	0.0006164
Reduced Graphene Oxide/Nickel	7.83	102	$9.459e^{-7}$	0.000315
Reduced Graphene Oxide/Cobalt	8.121	20.35	$1.513e^{-6}$	0.0000537

Table 5.4 shows an overall comparative analysis of different electrode materials for their electrochemical properties in supercapacitor with the prepared materials (reduced graphene oxide/ cobalt/ nickel/ copper. The incorporation of rGO in copper, cobalt and nickel based MOF enhances the overall surface area of electrode material and improves the conductivity.

TABLE 5.4: Comparative analysis of electrochemical properties of prepared electrocatalysts with already reported materials for the supercapacitor

Sr.No	**Material**	**Specific Capacitance (F/g)**	**Energy Density (Wh/Kg)**	**(Ref.)**
1	Polyamide/rGO	187	6.5	[107]
2	Sulphurized graphene	76	7.4	[108]
3	Nanoporous Carbon/ Cobalt Sulfide	159	5.5	[102]
4.	Activated carbon nanotube	145	4.7	[109]
5.	Porous 3D interconnected carbon framework	65	12.0	[110]
6.	Ultrafine Co_3O_4 nanocrystal electrode	172	3.0	[111]
7.	N-doped carbon nanofiber	195	6.0	[112]
8.	Graphene/MnO2/CNTs	61	8.9	[113]
9.	N,S-doped activated carbon from Elm Flower	62	12.4	[114]
10.	Reduced Graphene oxide/copper	29	2.19	[Current study]
11.	Reduced Graphene oxide/nickel	94	7.47	[Current study]
12.	Reduced Graphene oxide/cobalt	204	16.25	[Current study]

Chapter 6

Conclusions and Future Prospects

This chapter covers the summary of overall research work vis-à-vis synthesis, characterization and electrochemical analysis of prepared electrode material in Section 6.1. The second Section 6.2, highlights future prospects regarding supercapacitor research that may further improve the performance of these energy storage devices in the near future.

6.1 Conclusions

Reduced graphene oxide composites with cobalt, nickel and copper have been synthesized by using metal precursors and benzene tricarboxylic acid (BTC) as linkers reported via solvothermal method. It was observed that the incorporation of rGO increases the surface area and enhances the conductive properties of prepared catalysts. The surface morphology of prepared samples and the presence of specific elements and functional groups were confirmed by various techniques such as SEM. The electrochemical analysis was performed via cyclic voltammetry, electrochemical impedance spectroscopy and chronopotentiometry. Among all synthesized composites electrode materials rGO/cobalt exhibits high specific capacitance up

to 204 F/g and an energy density of 16.25 Wh/kg in 2M KOH. Reduced graphene oxide /nickel (show 94 F/g specific capacitance and 7.47 Wh/kg of energy density) and reduced graphene oxide/ copper (show 29 F/g of specific capacitance and 2.19 Wh/kg of energy density) illustrated low activity in contrast to reduced graphene oxide/cobalt. Graphene oxide/cobalt/nickel and copper capacitance characteristics are mainly directed via Faradaic redox reaction of cobalt, nickel and copper cation and attributed to the redox reactions of $Co^{2+}/Co^{3+}/Co^{4+}$ Cu^{2+}/Cu^{3+} *and* Ni^{2+}/Ni^{3+} over electrochemical development. Moreover, the impedance study of prepared samples shows correspondence with specific capacitance results. Reduced graphene oxide/copper show charge transfer resistance that is up to 46.97 Ω and other two samples, reduced graphene oxide/nickel and reduced graphene oxide/cobalt shows charge transfer resistance upto 102Ω and 20.35 Ω respectively.

6.2 Future Prospects

Though this synthesis method for electrode material is very efficient in terms of cost and easiness, improvement in the quality of graphene based substances still needs further research. To accomplish this, novel preparation techniques can be investigated like treatment with plasma, irradiation, thermal treatment processes and chemical activation methods to name a few. Certain carbon based organic materials which are derived from bio-based origin ought to have been considered due to their regular and intrinsic porosity found in their structure and easy availability in nature. It is also essential to accomplish the stability factor in the electrochemical process along with the economical aspect and high performance of the electrode materials in supercapacitors. In the research area of the supercapacitor, replacements, as well as advancements concerning fabrication of device, its electrode material devising, variety in electrolyte medium and packaging technique is the focus of the future investigation. In the proximate future, it is pretty achievable that a supercapacitor device having as good as energy density can be presented in the market which is comparable to the presently available lithium-ion battery systems.

Bibliography

[1] M. S. Halper and J. C. Ellenbogen, "Supercapacitors: A brief overview,", pp. 1-34, 2006, The MITRE Corporation, McLean, Virginia, USA.

[2] D. Qu, "Studies of the activated carbons used in double-layer supercapacitors," *Journal of Power Sources*, vol. 109, no. 2, pp. 403-411, 2002, Elsevier.

[3] J. Fernández, T. Morishita, M. Toyoda, M. Inagaki, F. Stoeckli, and T. A. Centeno, "Performance of mesoporous carbons derived from poly (vinyl alcohol) in electrochemical capacitors," *Journal of Power Sources*, vol. 175, no. 1, pp. 675-679, 2008, Elsevier.

[4] C. Liu, Z. Yu, D. Neff, A. Zhamu, and B. Z. Jang, "Graphene-based supercapacitor with an ultrahigh energy density," *Nano letters*, vol. 10, no. 12, pp. 4863-4868, 2010, American Chemical Society.

[5] B. E. Conway, Electrochemical Supercapacitors, and Fundamentals, "*Kluwer Academic and Plenum Publishers*," 1999, New York.

[6] S. Vivekchand, C. S. Rout, K. Subrahmanyam, A. Govindaraj, and C. Rao, "Graphene-based electrochemical supercapacitors," *Journal of Chemical Sciences*, vol. 120, no. 1, pp. 9-13, 2008, Spriger.

[7] A. Burke, "Ultracapacitors: why, how, and where is the technology," *Journal of Power Sources*, vol. 91, no. 1, pp. 37-50, 2000, Elsevier.

[8] X. Zhao, , H.Tian, M. Zhu, K. Tian, J. J. Wang, F. Kang, and R. A. Outlaw, "Carbon nanosheets as the electrode material in supercapacitors," *Journal of Power Sources*, vol. 194, no. 2, pp. 1208-1212, 2009, Elsevier.

[9] B. E. Conway, Electrochemical supercapacitors: scientific fundamentals and technological applications. 2013, *Springer Science & Business Media*.

[10] B. Babakhani and D. G. Ivey, "Improved capacitive behavior of electrochemically synthesized Mn oxide/PEDOT electrodes utilized as electrochemical capacitors," *Electrochimica Acta*, vol. 55, no. 12, pp. 4014-4024, 2010, Elsevier.

[11] J. Garche, C. K. Dyer, P. T. Moseley, Z. Ogumi, D. A. Rand, and B. Scrosati, Encyclopedia of electrochemical power sources. *Newnes*, 2013, Elsevier.

[12] H. Chen, Y. Ding, Y. Li, X. Zhang, and C. Tan, "Air fuelled zero emission road transportation: A comparative study," *Applied Energy*, vol. 88, no. 1, pp. 337-342, 2011, Elsevier.

[13] S. Rashidi, J. A. Esfahani, and F. Hormozi, "Classifications of Porous Materials for Energy Applications," 2020, Elsevier.

[14] M. Jayalakshmi and K. Balasubramanian, "Simple capacitors to supercapacitors-an overview," *International Journal of Electrocheical. Science*, vol. 3, no. 11, pp. 1196-1217, 2008, ESG.

[15] A. Rudge, J. Davey, I. Raistrick, S. Gottesfeld, and J. P. Ferraris, "Conducting polymers as active materials in electrochemical capacitors," *Journal of Power Sources*, vol. 47, no. 1-2, pp. 89-107, 1994, Elsevier.

[16] Y. Zhang, H. Feng, X.Wu, L.Wang, A.Zhang, T.Xia, H. Dong, X. Li, and L.Zhang, "Progress of electrochemical capacitor electrode materials: A review," *International Journal of Hydrogen Energy*, vol. 34, no. 11, pp. 4889-4899, 2009, Elsevier.

[17] C. Arbizzani, M. Mastragostino, and F. Soavi, "New trends in electrochemical supercapacitors," *Journal of Power Sources*, vol. 100, no. 1-2, pp. 164-170, 2001, Elsevier.

[18] C. Peng, S. Zhang, D. Jewell, and G. Z. Chen, "Carbon nanotube and conducting polymer composites for supercapacitors," *Progress in Natural Science*, vol. 18, no. 7, pp. 777-788, 2008, Elsevier.

[19] W. G. Pell and B. E. Conway, "Peculiarities and requirements of asymmetric capacitor devices based on combination of capacitor and battery-type electrodes," *Journal of Power Sources*, vol. 136, no. 2, pp. 334-345, 2004, Elsevier.

[20] H. Li, L. Cheng, and Y. Xia, "A hybrid electrochemical supercapacitor based on a 5 V Li-ion battery cathode and active carbon," *Electrochemical and Solid State Letters*, vol. 8, no. 9, p. A433, 2005, The Electrochemical Society.

[21] X. Wang and J. Zheng, "The optimal energy density of electrochemical capacitors using two different electrodes," *Journal of the Electrochemical Society*, vol. 151, no. 10, p. A1683, 2004, The Electrochemical Society.

[22] R. Wang, M. Yao, and Z. J. I. Niu, "Smart supercapacitors from materials to devices," *InfoMat*, vol. 2, no. 1, pp. 113-125, 2020, Wiley Online Library.

[23] L. Liu, H. Zhao, and Y. J. I. Lei, "Advances on three-dimensional electrodes for micro-supercapacitors: a mini-review," *InfoMat*, vol. 1, no. 1, pp. 74-84, 2019, Wiley Online Library.

[24] W. K. Chee, H. N. Lim, Z. Zainal, N. M. Huang, I. Harrison, and Y. J. T. J. o. P. C. C. Andou, "Flexible graphene-based supercapacitors: a review," *The Journal of Physical Chemistry C*, vol. 120, no. 8, pp. 4153-4172, 2016, American Chemical Society.

[25] M. Arvani, J. Keskinen, D. Lupo, and M. J. J. o. E. S. Honkanen, "Current collectors for low resistance aqueous flexible printed supercapacitors," *Journal of Energy Storage*, vol. 29, p. 101384, 2020, Elsevier.

[26] Z. Zhu, S. Tang, J. Yuan, X. Qin, Y. Deng, R. Qu, G. M Haarberg, "Effects of various binders on supercapacitor performances," *International Journal of Electrochemical Science*, vol. 11, no. 10, pp. 8270-8279, 2016, ESG.

[27] SUN, X. Z., ZHANG, X., HUANG, B., & MA, Y. W. (2014). Effects of separator on the electrochemical performance of electrical double-layer capacitor and hybrid battery-supercapacitor. *Acta Physico-Chimica Sinica*, 30(3), 485-491.

[28] A. Schneuwly and R. Gallay, "Properties and applications of supercapacitors from the state-of-the-art to future trends," *In Proc. PCIM*, vol. 2000(June).

[29] R. Kötz and M. Carlen, "Principles and applications of electrochemical capacitors," *Electrochimica Acta*, vol. 45, no. 15-16, pp. 2483-2498, 2000, Elsevier.

[30] H.-C. Zhou, J. R. Long, and O. M. Yaghi, "Introduction to metal–organic frameworks," vol.112, pp. 673-674, 2012, *ACS Publications*.

[31] T. Rodenas, I. Luz, G. Prieto, B. Seoane, H. Miro, A. Corma, F. Kapteijn, Francesc X. Llabrés i Xamena, and J. Gascon., " Metal–organic framework nanosheets in polymer composite materials for gas separation," *Nature Materials*, vol. 14, no. 1, pp. 48-55, 2015, Nature Publication Group.

[32] A. Dhakshinamoorthy and H. Garcia, "Catalysis by metal nanoparticles embedded on metal–organic frameworks," *Chemical Society Reviews*, vol. 41, no. 15, pp. 5262-5284, 2012, Royal Society of Chemistry.

[33] A. Arshad, A. Karkamkar, Y. J Choi, N. Tsumori, E.Ronnebro, T. Autrey, H. Shioyama, and Q. Xu, "Immobilizing highly catalytically active Pt nanoparticles inside the pores of metal–organic framework: a double solvents approach," *Journal of the American Chemical Society*, vol. 134, no. 34, pp. 13926-13929, 2012, American Chemical Society.

[34] Y.-R. Lee, J. Kim, and W.-S. Ahn, "Synthesis of metal-organic frameworks: A mini review," *Korean Journal of Chemical Engineering*, vol. 30, no. 9, pp. 1667-1680, 2013, Springer New York LLC.

[35] J. Yang, P. Xiong, C. Zheng, H. Qiu, and M. Wei, "Metal–organic frameworks: a new promising class of materials for a high performance supercapacitor electrode," *Journal of Materials Chemistry A*, vol. 2, no. 39, pp. 16640-16644, 2014, Royal Society of Chemistry.

[36] O. Yaghi, H. Li, and T. Groy, "Construction of porous solids from hydrogen-bonded metal complexes of 1, 3, 5-benzenetricarboxylic acid," *Journal of the American Chemical Society*, vol. 118, no. 38, pp. 9096-9101, 1996, American Chemical Society..

[37] L. Kang, S.-X. Sun, L.-B. Kong, J.-W. Lang, and Y.-C. Luo, "Investigating metal-organic framework as a new pseudo-capacitive material for supercapacitors," *Chinese Chemical Letters*, vol. 25, no. 6, pp. 957-961, 2014, Elsevier.

[38] L. Chen, J. Bai, C. Wang, Y. Pan, M. Scheer, and X. You, "One-step solid-state thermolysis of a metal–organic framework: a simple and facile route to large-scale of multiwalled carbon nanotubes," *Chemical Communications*, no. 13, pp. 1581-1583, 2008, Royal Society of Chemistry.

[39] F. Israr, D. K. Kim, Y. Kim, and W. Chun, "Scope of various solvents and their effects on solvothermal synthesis of Ni-BTC," *Química Nova*, vol. 39, no. 6, pp. 669-675, 2016, Brazilian Society of Chemistry.

[40] F. Israr, D. Chun, Y. Kim, and D. K. Kim, "High yield synthesis of Ni-BTC metal–organic framework with ultrasonic irradiation: role of polar aprotic DMF solvent," *Ultrasonics Sonochemistry*, vol. 31, pp. 93-101, 2016, Elsevier.

[41] A. F. Jalbout, X.-H. Li, M. R. Hassan, and G. G. Hossain, "Construction of novel coordination polymers with simple ligands," *Transition Metal Chemistry*, vol. 33, no. 5, pp. 597-603, 2008, Kluwer Academic Publishers.

[42] S. M. Lloyd, L. B. Lave, and H. S. Matthews, "Life cycle benefits of using nanotechnology to stabilize platinum-group metal particles in automotive catalysts," *Environmental Science & Technology*, vol. 39, no. 5, pp. 1384-1392, 2005, American Chemical Society.

[43] D. J. Tranchemontagne, J. R. Hunt, and O. M. Yaghi, "Room temperature synthesis of metal-organic frameworks: MOF-5, MOF-74, MOF-177, MOF-199, and IRMOF-0," *Tetrahedron*, vol. 64, no. 36, pp. 8553-8557, 2008, Elsevier.

[44] S. SY and S. Chui, "MF. Lo, JPH Charmant, AG Orpen and ID Williams,"A chemically functionalizable nanoporous material [Cu3(TMA)2(H2O) 3]" *Science Science*, vol. 283, p. 1148, 1999, American Association for the Advancement of Science.

[45] S. S.-Y. Chui, S. M.-F. Lo, J. P. Charmant, A. G. Orpen, and I. D. Williams, "A chemically functionalizable nanoporous material [Cu3 (TMA)2 (H2O)3] n," *Science*, vol. 283, no. 5405, pp. 1148-1150, 1999, American Association for the Advancement of Science.

[46] E. Biemmi, S. Christian, N. Stock, and T. Bein, "High-throughput screening of synthesis parameters in the formation of the metal-organic frameworks MOF-5 and HKUST-1," *Microporous and Mesoporous Materials*, vol. 117, no. 1-2, pp. 111-117, 2009, Elsevier.

[47] Z.Q. Li, L. G.Qiu, T. Xu, Y. Wu, W. Wang, Z. Y. Wu, and X.Jiang, "Ultrasonic synthesis of the microporous metal–organic framework Cu3(BTC)2 at ambient temperature and pressure: an efficient and environmentally friendly method," *Materials Letters*, vol. 63, no. 1, pp. 78-80, 2009, Elsevier.

[48] Y.K. Seo, G. Hundal, I.T. Jang, Y. K Hwang, C. H. Jun, J.S. Chang," Microwave synthesis of hybrid inorganic–organic materials including porous Cu3 (BTC) 2 from Cu (II)-trimesate mixture" *Microporous and Mesoporous Materials*, vol. 119, pp. 331-337, 2009, Elsevier.

[49] B. C. Smith, "Fundamentals of Fourier transform infrared spectroscopy," 2011, *CRC Press.*

[50] L. Reimer, Scanning electron microscopy: physics of image formation and microanalysis 2013 (vol. 36) Springer.

[51] M. Eckert, "Max von Laue and the discovery of X-ray diffraction in 1912," *Annalen der Physik*, vol. 524, no. 5, pp. A83-A85, 2012, Wiley-VCH.

[52] B. E. Warren, "X-ray Diffraction," 1990, Courier Corporation.

[53] U. Holzwarth and N. Gibson, "The Scherrer equation versus the'Debye-Scherrer equation," *Nature Nanotechnology*, vol. 6, no. 9, p. 534, 2011, Nature Research.

[54] X. Yan, X. Li, Z. Yan, and S. J. A. s. s. Komarneni, "Porous carbons prepared by direct carbonization of MOFs for supercapacitors," *Applied Surface Science*, vol. 308, pp. 306-310, 2014, Elsevier.

[55] X. Y. Hou, X. L. Yan, X. Wang, and Q. G. J. J. o. S. S. C. Zhai, "Tuning the porosity of mesoporous NiO through calcining isostructural Ni-MOFs toward supercapacitor applications," *Journal of Solid State Chemistry*, vol. 263, pp. 72-78, 2018, Elsevier.

[56] T. Purkait, G. Singh, D. Kumar, M. Singh, and R. S. J. S. r. Dey, "High-performance flexible supercapacitors based on electrochemically tailored three-dimensional reduced graphene oxide networks," *Scientific Reports*, vol. 8, no. 1, pp. 1-13, 2018, Nature Research.

[57] S. Liu, W. Yue, C. Zhang, D. Du, and X. Yang, "Enhanced lithium storage properties of graphene-based metal oxides by coating with amorphous TiO2 nanofilms," *Journal of Alloys and Compounds*, vol. 769, pp. 293-300, 2018, Elsevier.

[58] W. Yue, Yue, S. Jiang, W. Huang, Z. Gao, J. Li, Y. Ren, X. Zhao, and X. Yang, "Sandwich-structural graphene-based metal oxides as anode materials for lithium-ion batteries," *Journal of Materials Chemistry A*, vol. 1, no. 23, pp. 6928-6933, 2013, Royal Society of Chemistry.

[59] W. Zhang, Y. Zeng, N. Xiao, H. H. Hng, and Q. Yan, "One-step electrochemical preparation of graphene-based heterostructures for Li storage," *Journal*

of Materials Chemistry, vol. 22, no. 17, pp. 8455-8461, 2012, Royal Society of Chemistry.

[60] A. A. AbdelHamid, X. Yang, J. Yang, X. Chen, and J. Y. Ying, "Graphene-wrapped nickel sulfide nanoprisms with improved performance for Li-ion battery anodes and supercapacitors," *Nano Energy*, vol. 26, pp. 425-437, 2016, Elsevier.

[61] X. Chen, Chen, X. Xu, Z. Yang, Z. Liu, L. Zhang, X. Xu, Y. Chen, and S. Huang. "Sulfur-doped porous reduced graphene oxide hollow nanosphere frameworks as metal-free electrocatalysts for oxygen reduction reaction and as supercapacitor electrode materials," *Nanoscale*, vol. 6, no. 22, pp. 13740-13747, 2014, Royal Society of Chemistry.

[62] K.-J. Huang, J.-Z. Zhang, Y. Liu, and Y.-M. Liu, "Synthesis of reduced graphene oxide wrapped-copper sulfide hollow spheres as electrode material for supercapacitor," *International Journal of Hydrogen Energy*, vol. 40, no. 32, pp. 10158-10167, 2015, Elsevier.

[63] W. Liu, H. Niu, J. Yang, K. Cheng, K. Ye, K. Zhu, G. Wang, D. Cao, and J. Yan. "Ternary transition metal sulfides embedded in graphene nanosheets as both the anode and cathode for high-performance asymmetric supercapacitors," *Chemistry of Materials*, vol. 30, no. 3, pp. 1055-1068, 2018, American Chemical Society.

[64] G. Nie, X. Lu, J. Lei, L. Yang, and C. Wang, "Facile and controlled synthesis of bismuth sulfide nanorods-reduced graphene oxide composites with enhanced supercapacitor performance," *Electrochimica Acta*, vol. 154, pp. 24-30, 2015, Elsevier.

[65] R. Ramachandran, M. Saranya, P. Kollu, B. P. Raghupathy, S. K. Jeong, and A. N. Grace, "Solvothermal synthesis of Zinc sulfide decorated Graphene (ZnS/G) nanocomposites for novel Supercapacitor electrodes," *Electrochimica Acta*, vol. 178, pp. 647-657, 2015, Elsevier.

[66] W. Cai, T. Lai, J. Lai, H. Xie, L. Ouyang, J. Ye, and C. Yu. "Transition metal sulfides grown on graphene fibers for wearable asymmetric supercapacitors with high volumetric capacitance and high energy density," *Scientific Reports*, vol. 6, p. 26890, 2016, Nature Research.

[67] H. Tong, W. Bai, S. Yue, Z. Gao, L. Lu, L. Shen, S. Dong, J. Zhu, J. He, and X. Zhang, "Zinc cobalt sulfide nanosheets grown on nitrogen-doped graphene/-carbon nanotube film as a high-performance electrode for supercapacitors," *Journal of Materials Chemistry A*, vol. 4, no. 29, pp. 11256-11263, 2016, , Royal Society of Chemistry.

[68] A. Wang, H. Wang, S. Zhang, C. Mao, J. Song, H. Niu, B. Jin, and Y. Tian, "Controlled synthesis of nickel sulfide/graphene oxide nanocomposite for high-performance supercapacitor," *Applied Surface Science*, vol. 282, pp. 704-708, 2013 , Elsevier.

[69] X. Wang, S.-X. Zhao, L. Dong, Q.-L. Lu, J. Zhu, and C.-W. Nan, "One-step synthesis of surface-enriched nickel cobalt sulfide nanoparticles on graphene for high-performance supercapacitors," *Energy Storage Materials*, vol. 6, pp. 180-187, 2017, Elsevier.

[70] Z. S. Wu, Y.Z Tan, S. Zheng, S. Wang, K. Parvez, J. Qin, X. Shi "Bottom-up fabrication of sulfur-doped graphene films derived from sulfur-annulated nanographene for ultrahigh volumetric capacitance micro-supercapacitors," *Journal of the American Chemical Society*, vol. 139, no. 12, pp. 4506-4512, 2017, American Chemical Society.

[71] B. Xie, Y. Chen, M. Yu, T. Sun, L. Lu, T. Xie, Y. Zhang, and Y. Wu. "Hydrothermal synthesis of layered molybdenum sulfide/N-doped graphene hybrid with enhanced supercapacitor performance," *Carbon*, vol. 99, pp. 35-42, 2016, Elsevier.

[72] Z. Xing, Q. Chu, X. Ren, J. Tian, A. M. Asiri, K. A. Alamry, A. O. Al-Youbi, and X. Sun "Biomolecule-assisted synthesis of nickel sulfides/reduced

graphene oxide nanocomposites as electrode materials for supercapacitors," *Electrochemistry communications*, vol. 32, pp. 9-13, 2013, Elsevier.

[73] Yang, Juan, Chang Yu, Xiaoming Fan, Suxia Liang, Shaofeng Li, Huawei Huang, Zheng Ling, Ce Hao, and Jieshan Qiu "Electroactive edge site-enriched nickel–cobalt sulfide into graphene frameworks for high-performance asymmetric supercapacitors." *Energy & Environmental Science*, vol.9, pp. 1299-1307, 2016, Royal Society of Chemistry.

[74] X. Yu, Y. Kang, and H. S. Park, "Sulfur and phosphorus co-doping of hierarchically porous graphene aerogels for enhancing supercapacitor performance," *Carbon*, vol. 101, pp. 49-56, 2016, Elsevier.

[75] H. Zhang, X. Yu, D. Guo, B. Qu, M. Zhang, Q. Li, and T.Wang. "Synthesis of bacteria promoted reduced graphene oxide-nickel sulfide networks for advanced supercapacitors," *ACS Applied Materials & Interfaces*, vol. 5, no. 15, pp. 7335-7340, 2013, American Chemical Society.

[76] P. C. Banerjee, D. E. Lobo, R. Middag, W. K. Ng, M. E. Shaibani, and M. Majumder, "Electrochemical capacitance of Ni-doped metal organic framework and reduced graphene oxide composites: more than the sum of its parts," *ACS Applied Materials & Interfaces*, vol. 7, no. 6, pp. 3655-3664, 2015, American Chemical Society.

[77] X. Cao, , B. Zheng, W. Shi, J. Yang, Z. Fan, Z. Luo, X. Rui, B. Chen, Q. Yan, and H. Zhang, "Reduced graphene oxide-wrapped MoO3 composites prepared by using metal–organic frameworks as precursor for all-solid-state flexible supercapacitors," *Advanced Materials*, vol. 27, no. 32, pp. 4695-4701, 2015, Willey-VCH.

[78] D. Fu, H. Li, X.-M. Zhang, G. Han, H. Zhou, and Y. Chang, "Flexible solid-state supercapacitor fabricated by metal-organic framework/graphene oxide hybrid interconnected with PEDOT," *Materials Chemistry and Physics*, vol. 179, pp. 166-173, 2016, Elsevier.

[79] P. Srimuk, S. Luanwuthi, A. Krittayavathananon, and M. Sawangphruk, "Solid-type supercapacitor of reduced graphene oxide-metal organic framework composite coated on carbon fiber paper," *Electrochimica Acta*, vol. 157, pp. 69-77, 2015, Elsevier.

[80] L. Wang, T. Wei, L. Sheng, L. Jiang, X. Wu, Q. Zhou, B. Yuan, J. Yue, Z. Liu, and Z. Fan, "Brick-and-mortar" sandwiched porous carbon building constructed by metal-organic framework and graphene: Ultrafast charge/discharge rate up to 2 V s- 1 for supercapacitors," *Nano Energy*, vol. 30, pp. 84-92, 2016, Elsevier.

[81] D. Sheberla, J. C. Bachman, J. S. Elias, C.-J. Sun, Y. Shao-Horn, and M. Dincă, "Conductive MOF electrodes for stable supercapacitors with high areal capacitance," *Nature Materials*, vol. 16, no. 2, pp. 220-224, 2017, Nature Publishing Group.

[82] R. Díaz, M. G. Orcajo, J. A. Botas, G. Calleja, and J. Palma, "Co8-MOF-5 as electrode for supercapacitors," *Materials Letters*, vol. 68, pp. 126-128, 2012, Elsevier.

[83] Y. Yan, P. Gu, S. Zheng, M. Zheng, H. Pang, and H. Xue, "Facile synthesis of an accordion-like Ni-MOF superstructure for high-performance flexible supercapacitors," *Journal of Materials Chemistry A*, vol. 4, no. 48, pp. 19078-19085, 2016, Royal Society of Chemistry.

[84] Meng, F. L., Guo, Z., & Huang, X. J. (2015). Graphene-based hybrids for chemiresistive gas sensors. *TrAC Trends in Analytical Chemistry*, 68, 37-47.

[85] S. Gadipelli and Z. Guo, "Postsynthesis annealing of MOF-5 remarkably enhances the framework structural stability and CO2 uptake," *Chemistry of Materials*, vol. 26, no. 22, pp. 6333-6338, 2014, American Chemical Society.

[86] W. S. Hummers Jr and R. E. Offeman, "Preparation of graphitic oxide," *Journal of the American Chemical Society*, vol. 80, no. 6, pp. 1339-1339, 1958, American Chemical Society.

[87] Z.-S. Wu, W. Ren, L. Gao, B. Liu, C. Jiang, and H.-M. Cheng, "Synthesis of high-quality graphene with a pre-determined number of layers," *Carbon*, vol. 47, no. 2, pp. 493-499, 2009, Elsevier.

[88] A. Thakur, S. Kumar, and V. Rangra, "Synthesis of reduced graphene oxide (rGO) via chemical reduction," in *AIP Conference Proceedings*, vol. 1661, no. 1, p. 080032, 2015, American Institute of Physics.

[89] S. Lin, Z. Song, G. Che, A. Ren, P. Li, C. Liu, and J. Zhang, "Adsorption behavior of metal–organic frameworks for methylene blue from aqueous solution," *Microporous and Mesoporous Materials*, vol. 193, pp. 27-34, 2014, Elsevier.

[90] L. Yaqoob, T. Noor, N. Iqbal, H. Nasir, and N. Zaman, "Development of Nickel-BTC-MOF-Derived Nanocomposites with rGO Towards Electrocatalytic Oxidation of Methanol and Its Product Analysis," *Catalysts*, vol. 9, no. 10, p. 856, 2019, MDPI.

[91] T. Nguyen, C. L Luu, T. C Hoang, T. Nguyen, T. H Bui, P. H. D Nguyen, and T. P. P Thi, "Synthesis of MOF-199 and application to CO2 adsorption," *Advances in Natural Sciences.* Nanoscience and Nanotechnology (Online), vol. 4, no. 3, 2013,IOP Science.

[92] S. Homayoonnia and S. Zeinali, "Design and fabrication of capacitive nanosensor based on MOF nanoparticles as sensing layer for VOCs detection," *Sensors and Actuators B: Chemical*, vol. 237, pp. 776-786, 2016, Elsevier.

[93] G. Zeng, Y. Chen, L. Chen, P. Xiong, and M. Wei, "Hierarchical cerium oxide derived from metal-organic frameworks for high performance supercapacitor electrodes," *Electrochimica Acta*, vol. 222, pp. 773-780, 2016, Elsevier.

[94] Y. Zhang, Z. Zhu, K. Wong, R. Mi, J. Mei, and W. Lau "A green hydrothermal approach for the preparation of graphene/α-MnO_2 3D network as anode for lithium ion battery," *Electrochimica Acta*, vol. 108, pp. 465-471, 2013, Elsevier.

[95] S. Jabarian and A. Ghaffarinejad, "Electrochemical Synthesis of NiBTC Metal Organic Framework Thin Layer on Nickel Foam: An Efficient Electrocatalyst for the Hydrogen Evolution Reaction," *Journal of Inorganic and Organometallic Polymers and Materials*, vol. 29, no. 5, pp. 1565-1574, 2019, Springer.

[96] K. Sun, L. Li, X. Yu, L. Liu, Q. Meng, F. Wang, and R. Zhang."Functionalization of mixed ligand metal-organic frameworks as the transport vehicles for drugs," *Journal of Colloid and Interface Science*, vol. 486, pp. 128-135, 2017, Elsevier.

[97] L. Hamidipour and F. Farzaneh, "Cobalt metal organic framework as an efficient heterogeneous catalyst for the oxidation of alkanes and alkenes," Reaction Kinetics, *Mechanisms and Catalysis*, vol. 109, no. 1, pp. 67-75, 2013, Springer.

[98] B. F. Machado and P. Serp, "Graphene-based materials for catalysis," *Catalysis Science & Technology*, vol. 2, no. 1, pp. 54-75, 2012.

[99] Y. Li, K. Zhou, M. He, and J. Yao, "Synthesis of ZIF-8 and ZIF-67 using mixed-base and their dye adsorption," *Microporous and Mesoporous Materials*, vol. 234, pp. 287-292, 2016, Elsevier.

[100] J. He, X. Lu, J. Yu, L. Wang, and Y. Song, "Hierarchical $Co(OH)_2$ nanostructures/glassy carbon electrode derived from Co(BTC) metal–organic frameworks for glucose sensing," *Journal of Nanoparticle Research*, vol. 18, no. 7, p. 184, 2016, Springer.

[101] S. Kumaraguru, R. Pavulraj, and S. Mohan, "Influence of cobalt, nickel and copper-based metal-organic frameworks on the corrosion protection of mild steel," *Transactions of the IMF*, vol. 95, no. 3, pp. 131-136, 2017, Taylor& Francis Online.

[102] X. Dong, L. Wang, D. Wang, C. Li, and J. J. L. Jin, "Layer-by-layer engineered Co–Al hydroxide nanosheets/graphene multilayer films as flexible

electrode for supercapacitor," *Lnagmuir*, vol. 28, no. 1, pp. 293-298, 2012, American Chemical Society.

[103] R. Ahmad, N. Iqbal, M. M. Baig, T. Noor, G. Ali, and I. H. J. E. A. Gul, "ZIF-67 derived nitrogen doped CNTs decorated with sulfur and Ni (OH)2 as potential electrode material for high-performance supercapacitors," *Electrochimica Acta*, vol. 364, p. 137147, 2020, Elsevier.

[104] R. Ahmad, N. Iqbal, and T. J. M. Noor, "Development of ZIF-Derived Nanoporous Carbon and Cobalt Sulfide-Based Electrode Material for Supercapacitor, *Material*, vol. 12, no. 18, p. 2940, 2019, MDPI.

[105] Z.-S. Wu, W. Ren, D.-W. Wang, F. Li, B. Liu, and H.-M. J. A. n. Cheng, "High-energy MnO2 nanowire/graphene and graphene asymmetric electrochemical capacitors," *ACS Nano*, vol. 4, no. 10, pp. 5835-5842, 2010, American Chemical Society.

[106] V. Augustyn, P. Simon, B. J. E. Dunn, and E. Science, "Pseudocapacitive oxide materials for high-rate electrochemical energy storage," *Energy and Environmental Science*, vol. 7, no. 5, pp. 1597-1614, 2014, Royal Society of Chemistry.

[107] T. Y. Kim, H. W Lee, M. Stoller, D. R. Dreyer, C. W. Bielawski, R. S. Ruoff, and K. S. Suh "High-performance supercapacitors based on poly (ionic liquid)-modified graphene electrodes," *ACS Nano* 5, vol. 5, no. 1, pp. 436-442, 2011, American Chemical Society.

[108] J. S. Shaikh, N. S. Shaikh, R. Kharade, S. A. Beknalkar, J. V. Patil, M. P. Suryawanshi, P. Kanjanaboos, C. K Hong, J. H Kim, and P. S. Patil." Symmetric supercapacitor: Sulphurized graphene and ionic liquid," *Journal of Colloid and Interface Science* , vol. 527, pp. 40-48, 2018, Elsevier.

[109] W. Chen, R. Rakhi, M. N. Hedhili, and H. N. J. J. o. M. C. A. Alshareef, "Shape-controlled porous nanocarbons for high performance supercapacitors," *Journal of Materials Chemistry A*, vol. 2, no. 15, pp. 5236-5243, 2014, Royal Society of Chemistry.

[110] A. Bello, F. Barzegar, D. Momodu, J. Dangbegnon, F. Taghizadeh, and N. J. E. A. Manyala, "Symmetric supercapacitors based on porous 3D interconnected carbon framework," *Electrochimica Acta*, vol. 51, pp. 386-392, 2015, Elsevier.

[111] X. Y. Liu, Y. Q. Gao, and G. J. N. Yang, "A flexible, transparent and super-long-life supercapacitor based on ultrafine Co3O4 nanocrystal electrodes," *Nanoscale*, vol. 8, no. 7, pp. 4227-4235, 2016, Royal Society of Chemistry.

[112] L.F. Chen, Z. H Huang, H. W Liang, W. T Yao, Z. Y Yu, and S. H Yu. "Flexible all-solid-state high-power supercapacitor fabricated with nitrogen-doped carbon nanofiber electrode material derived from bacterial cellulose," *Energy & Environmental Science*, vol. 6, no. 11, pp. 3331-3338, 2013, Royal Society of Chemistry.

[113] Y. Cheng, S. Lu, H. Zhang, C. V. Varanasi, and J. J. N. l. Liu, "Synergistic effects from graphene and carbon nanotubes enable flexible and robust electrodes for high-performance supercapacitors," *Energy & Environmental Science*, vol. 12, no. 8, pp. 4206-4211, 2012, Royal Society of Chemistry.

[114] H. Chen, F. Yu, G. Wang, L. Chen, B. Dai, and S. J. A. o. Peng, "Nitrogen and sulfur self-doped activated carbon directly derived from elm flower for high-performance supercapacitors," *ACS Omega*, vol. 3, no. 4, pp. 4724-4732, 2018, American Chemical Society.